

AD-A072 198

NAVAL OCEAN SYSTEMS CENTER SAN DIEGO CA
PERFORMANCE MEASURES FOR AN AUTOMATED NAVY TACTICAL SOUNDER SYS--ETC(U)

F/G 17/9

JUL 79 L E HOFF, R L MERK

UNCLASSIFIED

NOSC/TR-409

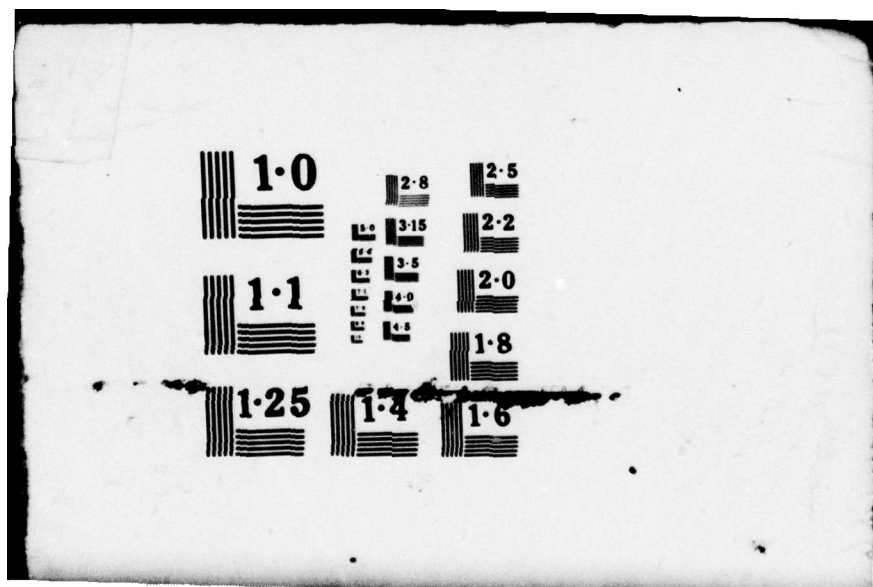
NL

| OF |
AD
A072198

NOSC



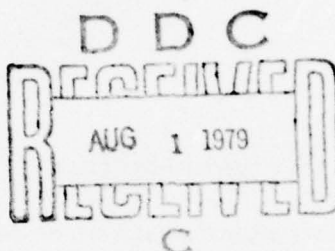
END
DATE
FILMED
9 - 79
DDC



LEVEL II
P2^{b5}

NOSC

NOSC TR 409



NOSC TR 409

Technical Report 409

ADA 072198
ADA 072199
**PERFORMANCE MEASURES FOR AN
AUTOMATED NAVY TACTICAL SOUNDER
SYSTEM (NTSS)**

LE Hoff
RL Merk

1 July 1979

Interim Report: July 1978 — July 1979

DDC FILE COPY

APPROVED FOR PUBLIC RELEASE; DISTRIBUTION UNLIMITED.

NAVAL OCEAN SYSTEMS CENTER
SAN DIEGO, CALIFORNIA 92152

79 08 1 025



NAVAL OCEAN SYSTEMS CENTER, SAN DIEGO, CA 92152

A N A C T I V I T Y O F T H E N A V A L M A T E R I A L C O M M A N D

SL GUILLE, CAPT, USN

Commander

HL BLOOD

Technical Director

ADMINISTRATIVE INFORMATION

The work presented in this report was completed by the Naval Ocean Systems Center, Surface/Ship Systems Division (Code 814) during the period July 1978 to July 1979.

Released by
CA Nelson, Head
Surface/Ship Systems Division

Under Authority of
HD Smith, Head
Communications Systems and
Technology Department

ACKNOWLEDGEMENTS

The authors thank Dr. George Dillard for providing valuable references and William Fay for editing and clarifying this report. We especially thank S. O. Rice for simplifying the computations of the probability of detection.

UNCLASSIFIED

SECURITY CLASSIFICATION OF THIS PAGE (When Data Entered)

REPORT DOCUMENTATION PAGE		READ INSTRUCTIONS BEFORE COMPLETING FORM
1. REPORT NUMBER NOSC Technical Report 409 (TR 409)	2. GOVT ACCESSION NO.	3. RECIPIENT'S CATALOG NUMBER
4. TITLE (and Subtitle) Performance Measures for an Automated Navy Tactical Sounder System (NTSS)		5. TYPE OF REPORT & PERIOD COVERED Interim: July 1978 July 1979
7. AUTHOR(s) LE Hoff RL Merk		6. PERFORMING ORG. REPORT NUMBER
9. PERFORMING ORGANIZATION NAME AND ADDRESS Naval Ocean Systems Center San Diego, California 92152		8. CONTRACT OR GRANT NUMBER(s)
11. CONTROLLING OFFICE NAME AND ADDRESS Naval Ocean Systems Center San Diego, California 92152		10. PROGRAM ELEMENT, PROJECT, TASK AREA & WORK UNIT NUMBERS (12) 51P
14. MONITORING AGENCY NAME & ADDRESS(if different from Controlling Office) (9) Interim rept. JUL 78 - JUL 79		12. REPORT DATE (14) 1 July 1979
		13. NUMBER OF PAGES 49
		15. SECURITY CLASS. (of this report) Unclassified
		16a. DECLASSIFICATION/DOWNGRADING SCHEDULE
16. DISTRIBUTION STATEMENT (of this Report) Approved for public release; distribution unlimited. (14) NOSC /TR-409/		
17. DISTRIBUTION STATEMENT (of the abstract entered in Block 20, if different from Report)		
18. SUPPLEMENTARY NOTES		
19. KEY WORDS (Continue on reverse side if necessary and identify by block number) list of L time delay coincidence test window duration threshold estimator sampling rate pulse resolution		
20. ABSTRACT (Continue on reverse side if necessary and identify by block number) Renewed interest by the Navy in the HF Radio Band has raised questions about the utility of the Navy Tactical Sounder System (NTSS) as part of the new systems of the 1980 and 1990 decades. Designed in the 1950's and used intermittently from 1960 to the present day, funding and support for the system are currently undergoing reevaluation, within the ELEX directed HF Improvement Program. In light of the recent advances in digital technology and communication theory, and the availability of Center internal funds, it seemed propitious to reexamine the fundamental signal design and processing algorithms (continued)		

UNCLASSIFIED

SECURITY CLASSIFICATION OF THIS PAGE(When Data Entered)

Block 20 (continued)

deriving

of the UPR-2 sounder receiver. The long term objective is a better receiver design easily implemented with micro-circuit technology. This report covers the first step in this process ~~it derives~~ performance measures related to signal detection and processing. Further analysis is left to the future, time and funds permitting.

The signal transmitted by the NTSS is essentially a channel probe meant to characterize the ionospheric path. The received signals contain information about path losses, time delays and frequency dispersion. From these basic parameters one can construct a channel model that can be used to estimate communication performance for any HF circuit. Channel performance metrics related to signal-to-noise ratio, error rate, synchronization and timing accuracy, multipath, fading, attenuation, and MUF and LUF can be extracted from the sounder receiver and used for management purposes. Thus the NTSS serves as a feedback link (or feed forward) for the express purpose of improving communications.

Three performance measures are evaluated: (1) the probability of detection; (2) the probability of false alarm; and (3) the timing resolution. The evaluation begins by describing a model of the Sounder receiver and a "list of L" detection algorithm. It is shown that a detection threshold set at the rms plus 6 dB noise level produces too high a false alarm rate. A threshold level of at least 3σ is required and an equivalent probability of detection of 0.99 requires a 13.6 dB signal-to-noise ratio. Since the rms value of the noise must be estimated using samples, the error in this estimate is related to window durations. A window duration of less than 3 milliseconds will degrade receiver performance below acceptable levels. The timing resolution of the peak amplitude of an arriving signal is ± 20 microseconds. This resolution, determined by the sampling rate, can be significantly improved with signal processing. For example, the peak of a 20 dB signal theoretically can be resolved within ± 4 microseconds.

Subsequent analysis should address performance measures for other parameters which can be extracted from the signals and which are useful for communications management.

Accession For	
NTIS GRA&I	
DDC TAB	
Unannounced	
Justification _____	
By _____	
Distribution/	
Availability Codes	
DIST	Avail and/or special

[Handwritten signature]

UNCLASSIFIED

SECURITY CLASSIFICATION OF THIS PAGE(When Data Entered)

SUMMARY

OBJECTIVE

The objective of this work is to examine the fundamental signal design and signal processing algorithms of the UPR-2 sounder receiver. This report derives performance measures related to signal detection and processing. The long term goal is to apply this knowledge to obtain a better receiver design easily implemented with microcircuit technology.

RESULTS

From an analysis of the basic detection algorithm of the UPR-2 receiver in SWGN, we conclude the following:

1. The minimum acceptable probability of false alarm should be 1.2×10^{-2} which requires a threshold noise value of 3 times the rms value. Using these values we can expect a probability of detection of 0.99 for an SNR of 13.6 dB. A detection threshold of 6-dB (2 rms) above the rms value yields an unacceptable high rate of false alarms ($P_{FA} = 10^{-1}$).
2. Using a sampling window of 3 milliseconds or less results in substantial loss in SNR due to errors in the rms estimate. To restrict the loss to less than 0.5 dB, a sampling window greater than 10.2 milliseconds is required for a P_D of 0.99.
3. Under the assumptions of signal and receiver bandwidths, 40-microsecond samples should allow time resolution of signal pulses to 20-microseconds. For optimum detection, a 4-microsecond resolution is possible under 20-dB SNR conditions.

RECOMMENDATIONS

In subsequent analysis additional complexity should be added until a reasonable representation of an HF ionospheric channel has been analyzed. Algorithms used by the AN/UPR-2 receiver should be analyzed under these circumstances and recommended improvement should be made. The following list of future work typifies important problems that should be solved.

1. Look at case where pulse time of arrival is not synchronous with sampling.
2. Examine practical algorithms for measuring time of arrival and compare to the case of optimum time of arrival estimate.
3. Extend these results to multipath and fading signals. Trade-off the list size, L, and the number of modes that can be resolved.
4. Examine other detection algorithms based on amplitude considerations.
5. Determine the effect of a jammer on non-SWGN.
6. Extraction of important system parameters, e.g.,
 - a. ionospheric path loss
 - b. synchronous time resolution
 - c. dispersion
 - d. best frequency, and
 - e. path quality.

CONTENTS

HISTORICAL PERSPECTIVE . . .	3
OBJECTIVES . . .	4
BACKGROUND . . .	4
APPROACH . . .	5
RESULTS . . .	10
CONCLUSIONS . . .	14
SUBSEQUENT ANALYSIS . . .	16
APPENDICES . . .	17

ILLUSTRATIONS

1. Relationship of NTSS and communications management . . . 4
2. Block diagram of sounder receiver . . . 5
3. Typical received envelopes for both sounder transmissions on a single channel . . . 6
4. Sounder receiver signal detection and processing algorithm . . . 7
5. Signal envelopes at matched filter output for large and small signal-to-noise ratios . . . 8
6. Example for the "list of L" detection algorithm . . . 9
7. Probability of false alarm for varying threshold settings . . . 11
8. Probability of detecting a single pulse using a "list of L" detection algorithm (L=3) . . . 11
9. Error in estimating the true rms value of the noise for various window durations . . . 12
10. Trade-off between sampling window duration and additional SNR required to maintain the desired P_D . . . 13
11. RMS error for optimum pulse resolution using a rectangular pulse with Gaussian rise and fall in SWGN . . . 15

HISTORICAL PERSPECTIVE

During the 1950 decade both the Navy and Air Force relied heavily on the HF radio band for long distance communications. Arguments for the use of oblique ionospheric sounders as aids to frequency management were sufficiently strong to result in the acquisition and operation of several sounders in the Atlantic and Pacific areas of high traffic. The sounder transmitters (AN/FPT-11) selected were high power, pulse modulation, which stepped through 80 frequencies from 2 to 32 MHz.

In the early 1960's the Navy installed transmitters at Honolulu, Philippine Islands, and Guam. Receivers (AN/UPR-2) were built and installed on capital ships, primarily aircraft carriers, and used on a regular basis for frequency management of ship-shore communication links. The Navy system of Pacific sounders became known as the Navy Tactical Sounder System (NTSS). This Center was charged with technical support of the system, most of which amounted to modifications and improvements to the receiving and transmitting equipments. In the latter half of the 1960's, funding support for the system declined. The Phillipines transmitter was abandoned and the supply of operable receivers began to dwindle. In the meantime the Air Force cut back its long distance HF circuits and turned off its Atlantic Sounder transmitters and offered them to the Navy for parts. Today, only the Honolulu and Guam transmitters are on the air and only a half dozen operable receivers exist. A transmitter, compatible with the Navy NTSS and installed by the French at Toulouse, has been in operation for more than a year.

The effectiveness of the NTSS as a practical system has received a mixed press from the users (Fleet) and system supporters (NAVTELCOM, ELEC). It has been the experience of this Laboratory that praise for the system came from knowledgeable communication officers aboard ship who were able to interpret the ionogram displays on the receiving set for useful frequency management purposes. During the Vietnam war, this Center did a brisk business in repairing receiving sets for communication officers aboard carriers which is a direct indication of their usefulness. The major complaints against the system were related primarily to training, only a skilled operator could use the system; and maintenance, parts for transmitters were scarce and shipboard personnel were unable to repair the receivers.

The Navy is in the process of taking another look at the NTSS from the standpoint of improving its effectiveness not only as a communications tool but also in the way it is supported logistically. Its potential as a direct input to communications management needs reexamination. A network of shore based sounder transmitters, located near communication receive stations, could provide the task force the means of automatic frequency management. By observing the sounder signals from all the (available) shore sites, the task force could automatically select and transmit on the best frequency not only for ship/shore links but also for ship/ship links. This procedure would optimize the signal-to-noise ratio and path quality for each message resulting in improved system availability and reliability. Automatic link management will be a fundamental part of the Naval Telecommunication System of the future.

The NTSS equipments, now approaching 20 years of age, were designed and built with the available technologies of the late 1950's. Since it is fundamentally a digital system, its modernization should bring with it significant improvements in performance, reduction

in size and cost of receiving equipments, and automation of many functions. With this in mind, this study is a deliberate reexamination of the original design with the intent of establishing performance measures for a modern (automated) NTSS.

OBJECTIVES

The overall objective of this project is to establish a set of performance measures for the NTSS of the 1980's which meet the expectations of the Naval Telecommunications Systems Architecture. We begin with a modest set of objectives - evaluation of the functions performed by the sounder receiver and operator which are subsets of the general function of frequency management.

In this report we confine our attention to the workings of the AN/UPR-2 sounder receiver as it was originally conceived. Our objective is to evaluate the basic signal detection algorithms and offer suggested improvements where warranted. Specifically, three performance measures are evaluated: (1) the probability of detection; (2) the probability of false alarm; and (3) the timing resolution of signal pulses.

BACKGROUND

The basic NTSS design calls for a number of transmitters interspersed within an ocean area to allow ships at sea to make good communications management decisions. This decision-making process and its relationship to the NTSS signals and receiving equipments are illustrated in figure 1. The function of the receiving equipments is to characterize the ionospheric channel by detecting and processing the signals. From this characterization communications management decisions can be made as to radio frequency, link terminations, antenna and radiated power, type of modulation for EW purposes, data rate, and timing and sync information. Only the functions performed by the receiving equipments will be analyzed in this report. Before proceeding, some refresher material on the signals generated by the NTSS transmitter is reviewed.

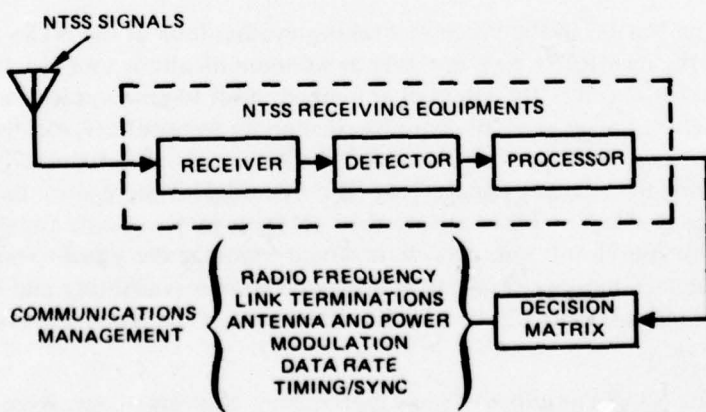


Figure 1. Relationship of NTSS and communications management.

The transmitter is a step frequency sounder that transmits pulses on 80 frequencies between 2 and 32 MHz in 16 seconds. Time between frequency steps is 200 milliseconds; however only the first 100 milliseconds on each frequency are used for channel sounding. The signal format consists of two pulses, 2.6 milliseconds long, spaced 50 milliseconds apart. Each pulse is a PSK modulated Barker sequence, consisting of 13 chips. Each chip is wave-shaped to reduce the spectrum outside the nominal bandwidth of 7.5 kHz. The chip waveform consists of a 20 microsecond Gaussian rise, a flat center portion for 160 microseconds, and a 20 microsecond fall. The transmit power is $30 \text{ kW} \pm 1 \text{ dB}$ into a vertical monopole antenna. Additional sounder specifications are summarized in Appendix A.

Implementation of a sounder receiver* is quite simple in concept. One implementation is shown in figure 2. The receiver front end is stepped along in unison with the transmitter and allowed to settle on each of the 80 channels long enough to receive the transmitted signals. The receiver has i and q channels containing a matched filter for the Barker code. This is followed by a squaring circuit. The two channels are then added, the square root taken, and the output is then sampled (40 microseconds) and buffered. Timing and sync signals are supplied to enable search windows to be opened at appropriate intervals and for establishing the time delay (ionospheric path) of received signals.

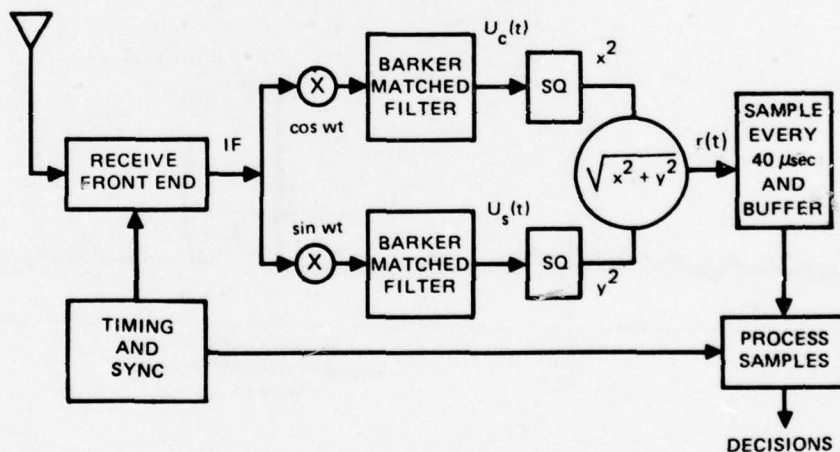


Figure 2. Block diagram of sounder receiver.

APPROACH

In this section we discuss the signal detection problem and present a "list of L" detection scheme for the multiple modes that may be present. The purpose is to establish a baseline performance measure of detecting nonfading sounder signals in stationary white Gaussian noise (SWGN). The three performance measures considered are: (1) the probability of detection; (2) the probability of false alarm; and (3) the pulse resolution and timing accuracy.

*Slack, Robert, Technical Description and Use of the AN/UPR-2(XN-1) Sounder Receiver; NELC TD 29; 17 April 1968.

We begin our discussion of the detection problem by examining the envelope of the output of the matched filter. Figure 3 illustrates two envelope samples (r_1 and r_2) received on one sounder channel separated by 50 milliseconds. Two signals plus noise are shown in each sample and are illustrative of a typical HF radio path containing multiple modes. In this example the search window is 8 milliseconds in duration.

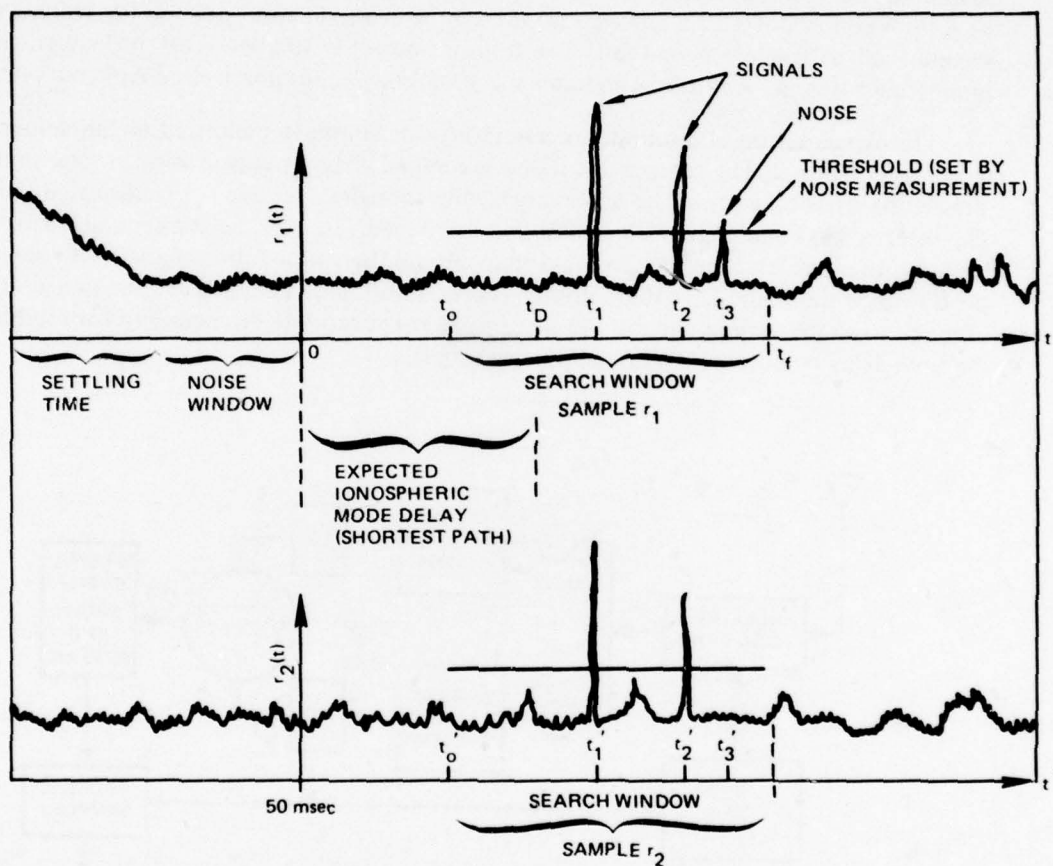


Figure 3. Typical received envelopes for both sounder transmissions on a single channel.

The first clue in identifying signals in noise is to assume that large envelope excursions are signal. The second is the time correlations of the signals in samples r_1 and r_2 . Since corresponding samples in r_1 and r_2 are separated by 50 milliseconds, a period too short for changes to occur in the ionospheric path, each signal sample should be a replica of each other. The noise on the other hand will have uncorrelated envelopes. Thus in figure 3 we see two envelope spikes easily identified as signals, and a noise spike not mistaken for a signal because no corresponding spike appears in sample r_2 at t'_3 . As long as the signals are strong, i.e., well above the background noise, it is easy to distinguish them and to mark their times of arrival, t_1 and t_2 . When the signals are weak, the ability to make a good decision is much more difficult and false alarms or missed messages (signals) will occur. With a threshold

noise level set as illustrated, the decision process will have few errors. In well behaved noise, as in stationary white Gaussian noise, a predetermined level can be easily established such that false alarm and missed messages are reasonable. In non-well behaved noise environments, as encountered in the HF band, the average noise level varies with time (non stationary) and has characteristically more spikes. Both of these conditions make the decision process more difficult.

Assuming that the signals and noise illustrated in figure 3 are typical, algorithms describing the detection and processing of the signals can be generated. One such algorithm is presented in figure 4. Briefly, the process begins with an estimate of the noise (rms), followed by the setting of a threshold, a list of L detection scheme, and finally an estimate of the time delay of each signal, its ionospheric mode and path loss.

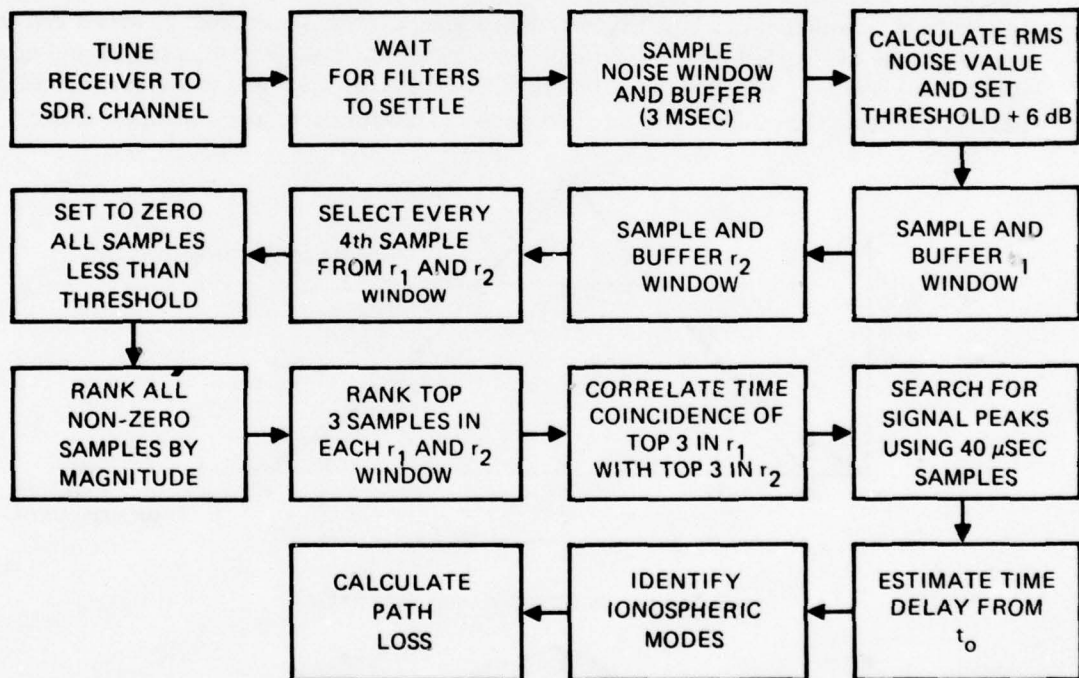


Figure 4. Sounder receiver signal detection and processing algorithm.

In estimating the rms value of the noise, buffered samples taken every 160 microseconds with a 3-millisecond window are used in the calculation. Samples separated by 160 microseconds are considered independent based upon the signal and filtered bandwidths of 7.5 kHz.

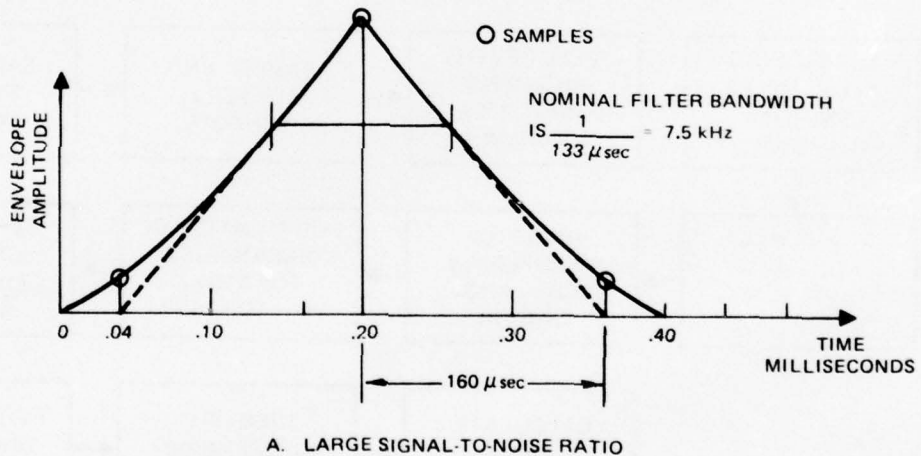
Denoting the independent sample values by r_i , where $r_i = \sqrt{x_i^2 + y_i^2}$ and the total

number of samples by N, the rms noise estimate, S, is computed by the following formula:

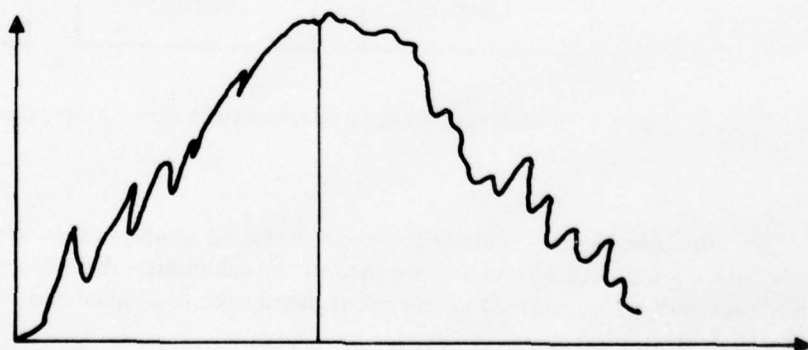
$$S = \sqrt{\frac{1}{N} \sum_{i=1}^N r_i^2} \quad . \quad (1)$$

With a noise buffer 3 milliseconds long, the number of independent samples for this interval is 22. As the noise buffer becomes longer, the rms noise measurement becomes more accurate. The accuracy of the rms measurement and the consequence of errors made in this measurement as a function of buffer size is given in the section on results.

For large values of signal-to-noise ratio the signal envelope out of the matched filter will look like that of figure 5-A (neglecting Barker code side lobes down 22 dB). If the signal peak coincides with one of the 160 microsecond samples, as shown, then the values on either side will be well down from the peak. If the peak does not coincide with one of the samples (a case to be considered in a later report), then a search for the peak must be made. For the non-ideal case of signal plus noise, the signal envelope may look like 5-B, a ragged and non-symmetric version of 5-A. For the purposes of this study we are going to assume that all signal peaks are separated by at least 160 microseconds and always occur at the sample values.



A. LARGE SIGNAL-TO-NOISE RATIO



B. SMALL SIGNAL-TO-NOISE RATIO

Figure 5. Signal envelopes at matched filter output for large and small signal-to-noise ratios.

A description of the "list of L" detection scheme ($L=3$) with an illustrative example follows. Let t_k denote an arbitrary independent sample time. A mode is declared at a particular time, t_k , only if: (1) a sample peak exceeds the threshold at t_k in both $r_1(t)$ and $r_2(t)$; and (2) the amplitude of the sample peak is ranked in the top 3 in both r_1 and in r_2 . Only samples above the threshold are ranked according to amplitude. Samples which fall below the threshold are set equal to zero.

This decision criterion is illustrated in figure 6 where we show ranked samples for both $r_1(t)$ and $r_2(t)$. Only the top three ranked samples are passed to the coincidence test. The results of the coincidence test indicate that modes are declared only at t_2 and t_5 .

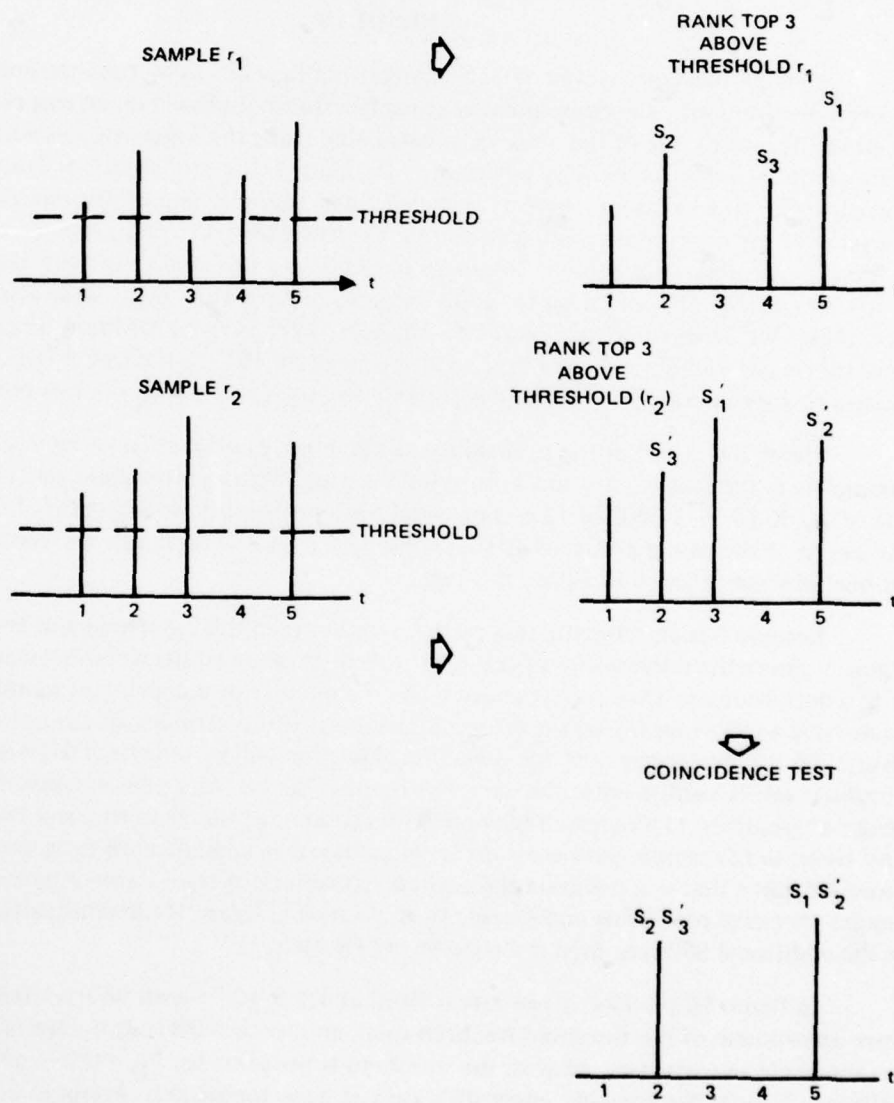


Figure 6. Example for the "list of L" detection algorithm.

Significant probabilities of this detection scheme, namely probability of false alarm (P_{FA}) and probability of detection (P_D), are derived in Appendices B and C respectively. The performance is given in the next section.

The last portion of the algorithm of figure 4 is concerned with identifying the time delay of the signals. When a mode is declared to occur at a sample time, t_k , finer spaced samples 40 microseconds apart on both sides of t_k are used to resolve the pulse peak and hence the time of arrival. The maximum error in determining where this peak occurs happens when the peak falls midway between two adjacent samples; the error in this case is 20 microseconds. In Appendix D this error will be shown to be significantly greater than the error due to small values of signal-to-noise ratio.

RESULTS

Since performance of the detection algorithm depends upon the threshold setting, we begin by evaluating the consequences of using a threshold based on an rms estimate of the noise. The rms value of the noise, S , is calculated using the noise samples within a 3-millisecond window as given by equation 1. In figure 7, the probability of false alarm is plotted for varying values of threshold settings. Since the rms value of the envelope equals the rms value of the input noise times $\sqrt{2}$, denote the rms value of the envelope by σ_o , i.e., $\sigma_o = \sigma\sqrt{2}$. A threshold setting of $2\sigma_o$ ($\sigma_o + 6$ dB) gives a probability of false alarm of 10^{-1} , clearly an unacceptable situation for good decision making. How many false alarms are acceptable? We believe one false alarm per sounder sweep is an upper limit. Since there are 80 channels per sounder sweep, a P_{FA} of approximately 10^{-2} per channel is dictated. This equates to approximately a threshold setting of $3\sigma_o$ or 9.5 dB above the rms noise estimate.

Figure 8 is a plot of the probability of detection as a function of signal-to-noise ratio parametric in false alarm rate and T , threshold setting. With the threshold set for a false alarm rate of 1.2×10^{-2} , a SNR of 13.6 is required for a probability of detection of 0.99. Thus for one sweep of the sounder through 80 channels with a SNR of 13.6 dB, we would expect to get one false alarm and one missed message.

Because S is an estimate, there is an error between the calculated and true rms value. Figure 9 shows the relationship of this error to the duration of the sampling window. Details of this derivation are given in Appendix E. As the number of independent samples increases (increasing window duration) the error will decrease. If our estimate of the noise is in error by several dB, the performance of the detection algorithm will be uncertain depending upon the threshold values used to enter the curves of figures 7 and 8. As a consequence, there are two design alternatives: (1) increase the window duration until the measured and true values are very close; or (2) sample during a short window duration and add a dB fudgefactor to the threshold value that will maintain the desired probability of false alarm. Alternative (1) could require excessive processing and storage time. Therefore figure 10 demonstrates the SNR lost or the additional SNR required if alternative (2) is used.

In figure 10 the false alarm rate is fixed at 1.2×10^{-2} with 98% confidence. Therefore since an estimate of the threshold has been used, an identical dB fudgefactor has been added to the threshold in each case. That is, the threshold is the same for $P_D = 0.99$ and $P_D = 0.90$, but SNR is different. Surprisingly, more dB's are lost using ambiguous threshold estimates at the lower SNR. This behavior is apparent from figure 8 by noting the larger horizontal distance

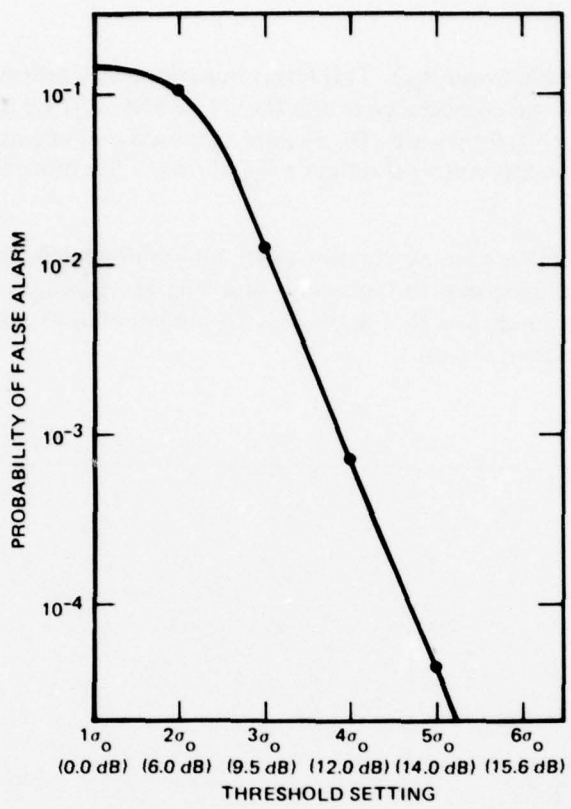


Figure 7. Probability of false alarm for varying threshold settings.

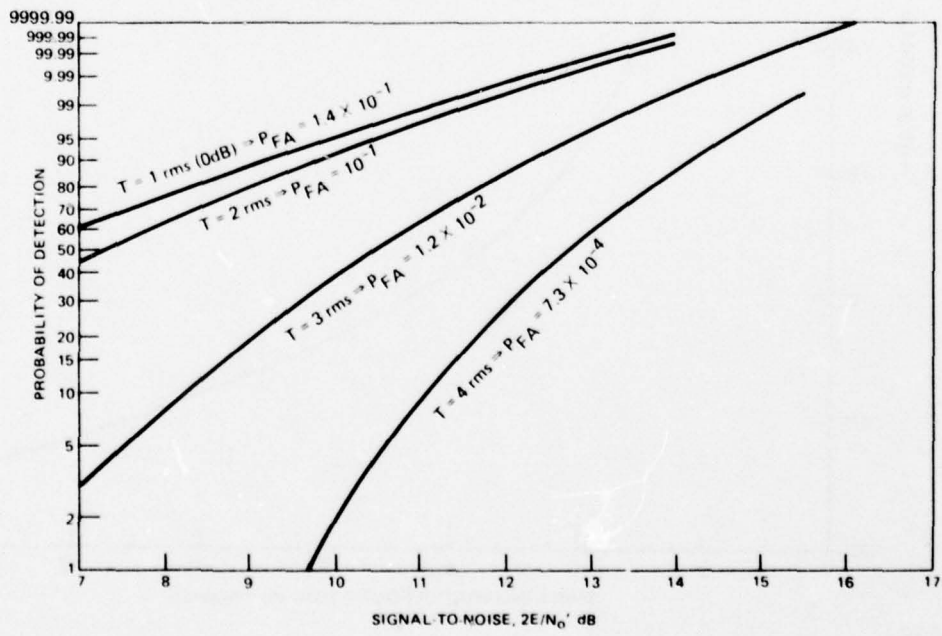


Figure 8. Probability of detecting a single pulse using a "list of L" detection algorithm ($L=3$).

between the curves at the lower P_D 's. This larger horizontal separation at low SNR is due to the sensitive nature of the coincidence test at these low SNR's. If we require the dB loss not to exceed 0.5 dB at a $P_D = 0.99$ (figure 10), a sampling window of at least 11 milliseconds is required; whereas if we attempt to maintain a P_D of only 0.90, more than 12 milliseconds would be required.

For short sampling window durations such as 4 milliseconds only 1.25 dB is lost at $P_D = 0.99$. Below 2 milliseconds the curves become very steep and this region should be avoided. Figure 10 also indicates that more than 14 milliseconds of sampling is necessary to reduce the loss to less than 0.1 dB.

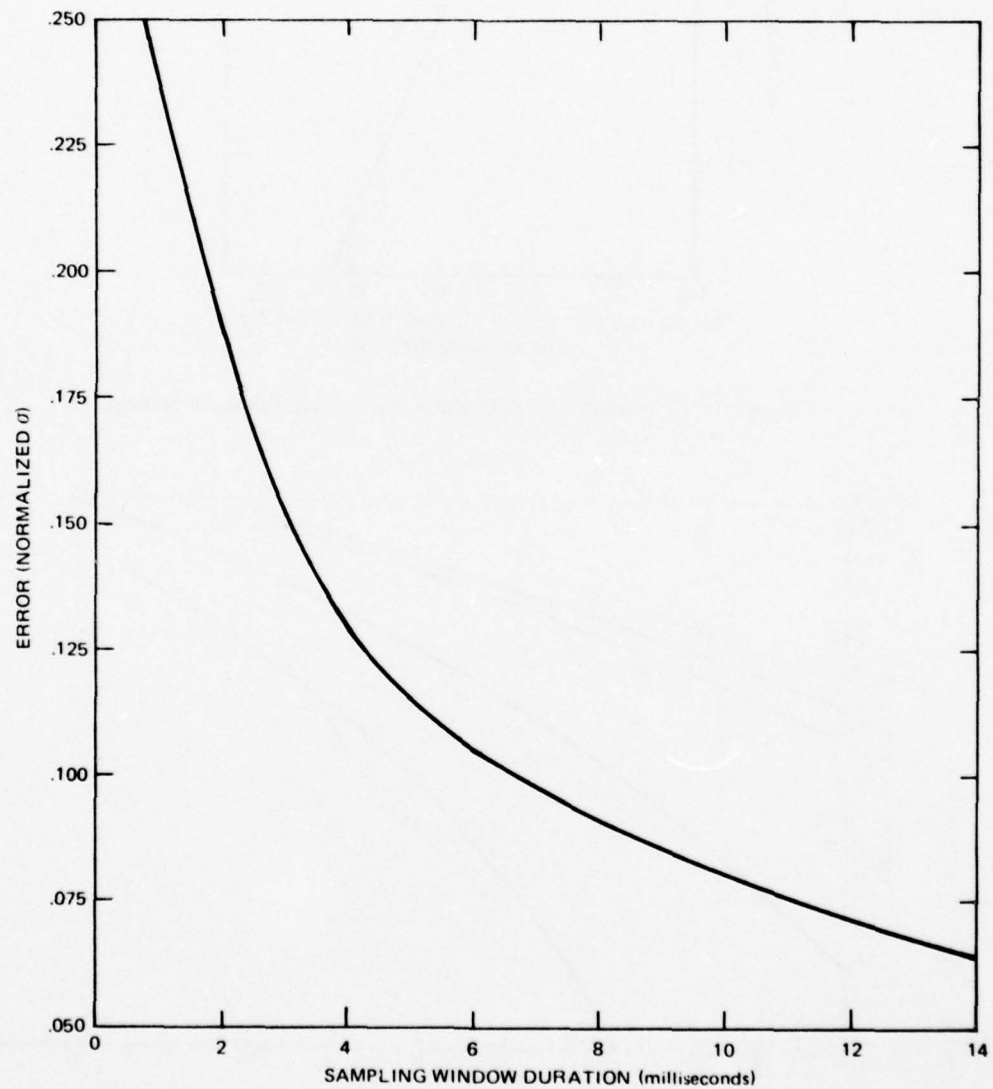


Figure 9. Error in estimating the true rms value of the noise for various window durations.

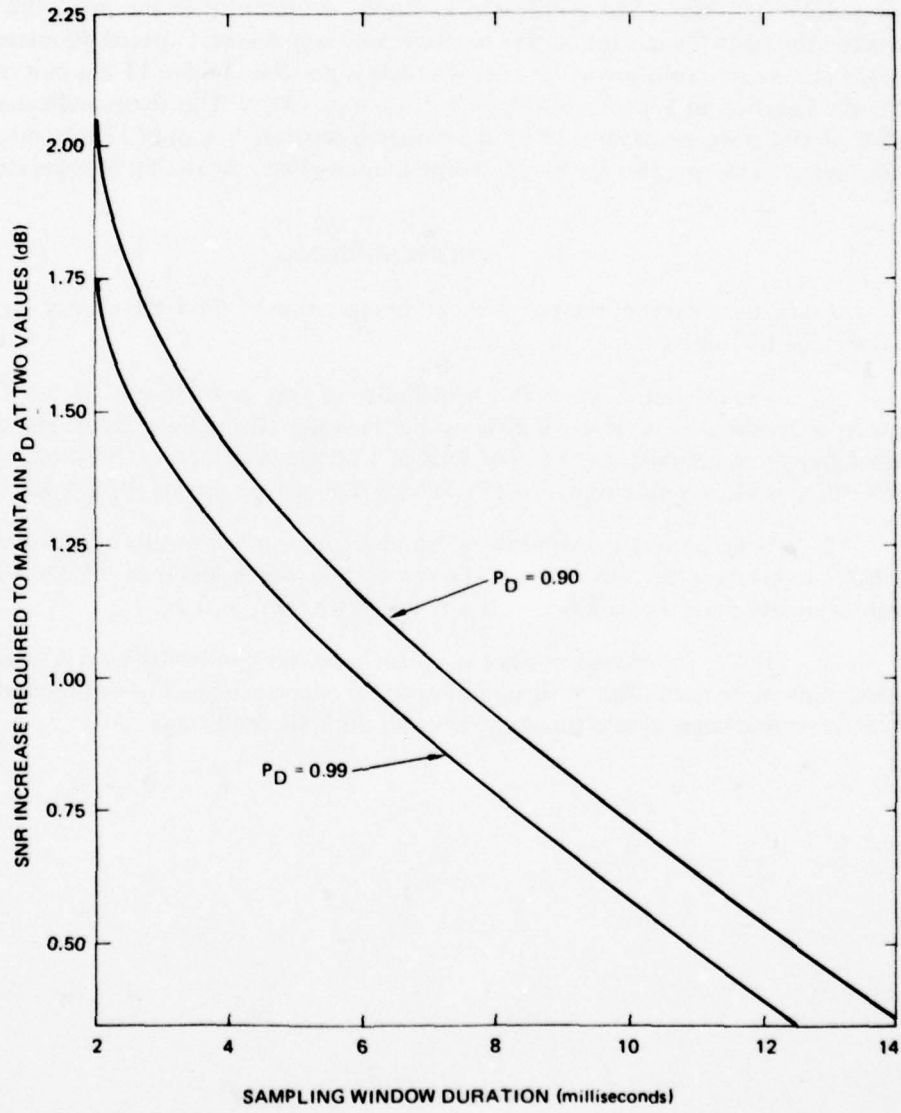


Figure 10. Trade-off between sampling window duration and additional SNR required to maintain the desired P_D . False alarm rate is fixed at 1.2×10^{-2} with 98% confidence.

Coincident with the problem in detection is the ability to resolve two signals which are separated in time. The problem here is the ability to resolve the peak of the arriving signal when this peak is corrupted by noise. That is, noise spikes which occur near the peak of the arriving signal when added with the signal at that point may be larger than the signal peak itself and therefore mistaken for the true peak. The optimum resolution of signal peaks corrupted by SWGN is derived in Appendix D for three different pulse shapes.

The results of Appendix D can be applied to the question of sample spacing for maximum pulse resolution in SWGN. Clearly if no noise is present then the closer the samples are taken the finer the resolution will be. Since our samples were spaced 40 microseconds apart, a minimum resolution of 20 microseconds is possible. Figure 11 is a plot of the rms error as a function of SNR for optimum detection in SWGN. This figure indicates that for a SNR of 10 dB we are capable of resolving signals separated by only 12 microseconds. Two ways of achieving this are by increasing the sampling rate and by interpolation methods.

CONCLUSIONS

From an analysis of the basic detection algorithm of the UPR-2 receiver in SWGN, we conclude the following:

1. The minimum acceptable probability of false alarm should be 1.2×10^{-2} which requires a threshold noise value of 3 times the rms value. Using these values we can expect a probability of detection of 0.99 for an SNR of 13.6 dB. A detection threshold of 6 dB (2 rms) above the rms value yields an unacceptable high rate of false alarms ($P_{FA} = 10^{-1}$).
2. Using a sampling window of 3 milliseconds or less results in substantial loss in SNR due to errors in the rms estimate. To restrict the loss to less than 0.5 dB, a sampling window greater than 10.2 milliseconds is required for a P_D of 0.99.
3. Under the assumptions of signal and receiver bandwidths, 40 microsecond samples should allow time resolution of signal pulses to 20 microseconds. For optimum detection, a 4 microsecond resolution is possible under 20 dB SNR conditions.

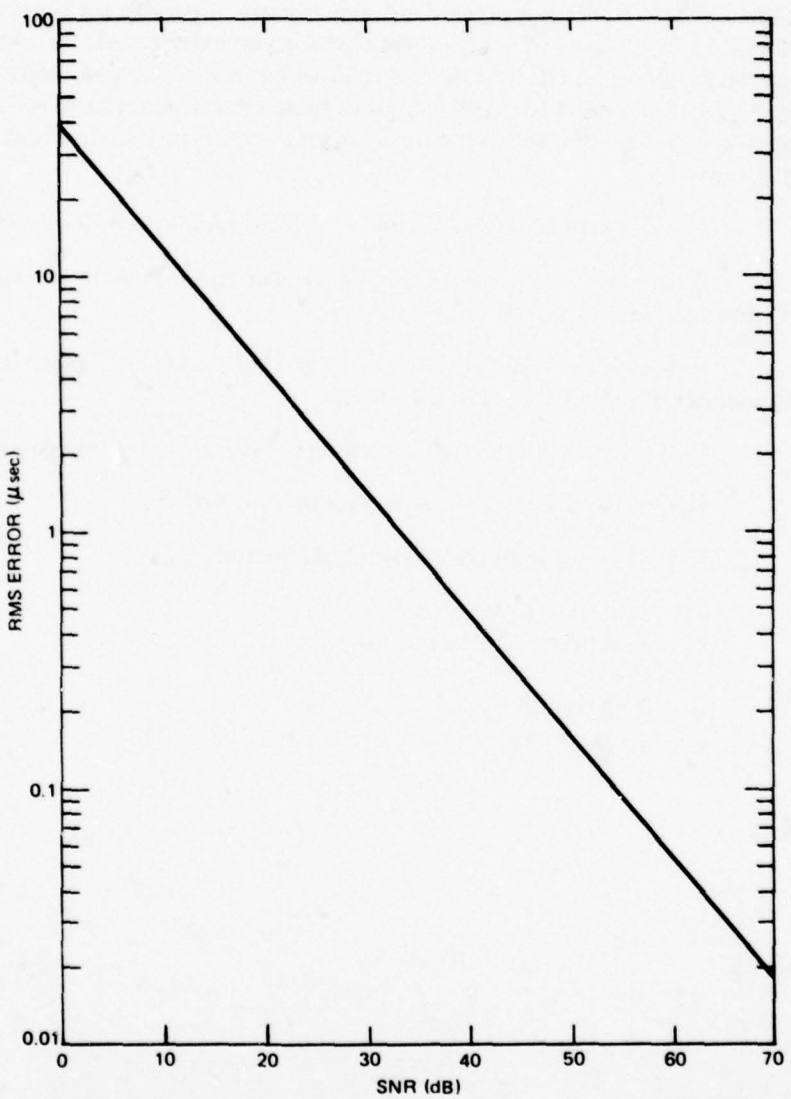


Figure 11. RMS error for optimum pulse resolution using a rectangular pulse with Gaussian rise and fall in SWGN.

SUBSEQUENT ANALYSIS

This report is the first step in estimating the performance of the sounder receiver. It was kept intentionally simple so that the basic performance could be estimated under ideal conditions—SWGN, nonfading signals and signals easily separable (in time) at the output of the matched filter. In subsequent analysis additional complexity should be added until a reasonable representation of an HF ionospheric channel has been analyzed. Algorithms used by the AN/UPR-2 receiver should be analyzed under these circumstances and recommended improvement should be made. The following list of future work typifies important problems that should be solved.

1. Look at case where pulse time of arrival is not synchronous with sampling.
2. Examine practical algorithms for measuring time of arrival and compare to the case of optimum time of arrival estimate.
3. Extend these results to multipath and fading signals. Trade-off the list size, L, and the number of modes that can be resolved.
4. Examine other detection algorithms based on amplitude considerations.
5. Determine the effect of a jammer on non-SWGN.
6. Extraction of important system parameters, e.g.,
 - a. ionospheric path loss
 - b. synchronous time resolution
 - c. dispersion
 - d. best frequency, and
 - e. path quality.

APPENDIX A
SOUNDER LINK SPECIFICATIONS

APPENDIX A SOUNDER LINK SPECIFICATIONS

This appendix is meant to provide a concise catalogue listing of pertinent specifications of the sounder. Most of this information has been gleaned from: Slack, Robert, "Technical Description and Use of the AN/UPR-2(XN-1) Sounder Receiver," NELC TD 29, 17 April 1968. Hence if further information is required, a thorough reading of this document is recommended.

1. 13 chips, 0.2 msec long, 2.6 msec total.
2. Nominal bandwidth is 7.5 kHz.
3. Absolute maximum PEP is 30 kw.
4. Absolute maximum pulse width is 3.2 ms.
5. 80 pulse pairs of barker signal.
6. Receiver N.F. 15 dB.
7. Combined NF of receiver and antenna (shipboard installation).

Frequency	N.F. dB
2	52
4	47
6	42
9	33
12 to 30	21

8. Sounder link algorithm
 - a. Find largest 3 pulses in 8 ms gate 1 and tag times.
 - b. Pair pulses over 50 ms \pm 40 μ sec for coincidence test.
 - c. Take first coincidence to set time and \pm 2.5 ms gate #2.
 - d. Take largest of coincidence pairs for power measurement.
 - e. Reject pulses less than 6 dB over noise outside gate #2.

9. Sounder frequency allocations

Band	Start Freq	Increment	Channels
2-4	2.075	100 kHz	20
4-8	4.150	200	20
8-16	8.300	400	20
16-32	16.600	800	20

10. Barker sequence

1,1,1,1,1,0,0,1,1,0,1,0,1

APPENDIX B
PROBABILITY OF FALSE ALARM

APPENDIX B PROBABILITY OF FALSE ALARM

A false alarm is an error made by saying a signal is present when in fact it is not. The purpose of this appendix is to determine the false alarm rate for the assumed detection criterion. This criterion employs the independent samples of two received envelopes, which we will denote by $r_1(t)$ and $r_2(t)$. In figure B1, $r(t)$ is general and represents either $r_1(t)$ or $r_2(t)$. We have assumed an 8 msec search window (sampling interval) with 7.5 kHz bandwidth. Hence there are 60 independent samples in $r(t)$. Since the probability of false alarm is determined by the threshold, we have set a variable threshold measured in numbers of the rms value.

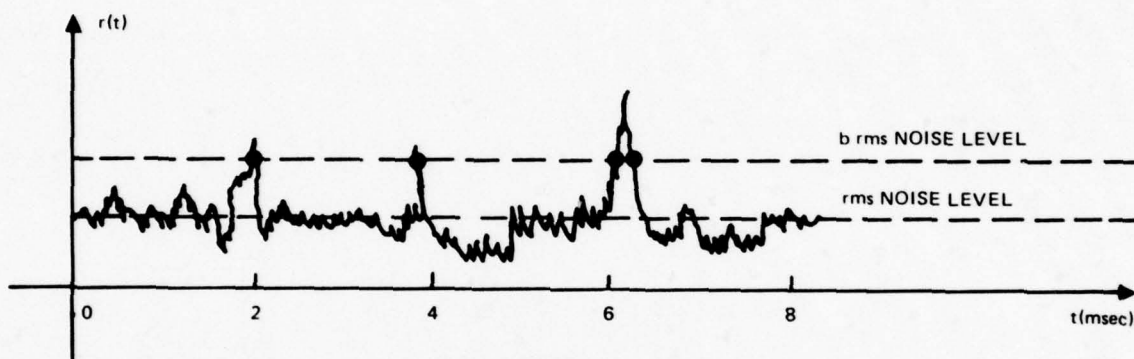


Figure B1. Received noise envelope.

The detection criterion is based on a coincidence test between the independent samples of $r_1(t)$ and the independent samples of $r_2(t)$. First, samples below the threshold are set equal to zero. Next, the non-zero samples are ranked from largest to smallest according to amplitude. Finally the top three ranked samples of $r_1(t)$ are compared with the top three ranked samples of $r_2(t)$. Only if there is a coincidence between one of the top three ranked samples of $r_1(t)$ and one of the top three ranked samples of $r_2(t)$, 50 msec later, will a detection be declared (a false alarm in the noise only case). Note, when there are less than three ranked samples in either $r_1(t)$ or $r_2(t)$, only ranked samples are used in the coincidence test.

Since the envelope, $r(t)$, is the envelope of a narrowband Gaussian process, the distribution of $r(t)$ is Rayleigh in the noise only case, therefore the probability that $r(t)$ at any particular sample time is greater than a given threshold, T , is given by equation B-1.

$$P_r \left\{ r > T \right\} = \int_T^{\infty} p(r) dr = e^{-T/\sigma} = p \quad (B-1)$$

where

$$p(r) = \frac{r}{\sigma^2} e^{-r^2/2\sigma^2}$$

If the threshold is set 6 dB above the rms noise level, i.e., $T = 2\sqrt{2}\sigma$, then

$P_r \left\{ r > 2\sqrt{2}\sigma \right\} = e^{-2\sqrt{2}} \approx 5.91 \times 10^{-2}$. Denoting the probability of a single sample exceeding the threshold by p , the total number of independent samples by N , and the number of samples exceeding the threshold out of the N independent samples by n , then by the binomial theorem the probability that n noise samples exceed the threshold is given in equation B-2.

$$P(n, N) = \binom{N}{n} p^n (1-p)^{N-n} = \frac{N!}{(N-n)! n!} p^n (1-p)^{N-n}. \quad (\text{B-2})$$

With the threshold set 6 dB above the rms noise level and the number of independent samples equal to 60, the probability that two noise values exceed the threshold $\approx 1.81 \times 10^{-1}$.

Define the event E_{ij} , given i and $j \leq 2$, as the event that i samples in $r_1(t)$ and j samples in $r_2(t)$ exceed the threshold. When either i or j are equal to three then the event E_{ij} is the event that three or more samples exceed the threshold for each index equal to three. Hence the probability of false alarm, P_{FA} , using the coincidence test of the top three ranked samples is:

$$\begin{aligned} P_{FA} &= \sum_{i=0}^3 \sum_{j=0}^3 P(\text{FA}/E_{ij}) P(E_{ij}) \\ &= \sum_{i=1}^3 \sum_{j=1}^3 P(\text{FA}/E_{ij}) P(E_{ij}), \end{aligned} \quad (\text{B-3})$$

where $P(\text{FA}/E_{ij})$ is the probability of false alarm conditioned on the event E_{ij} . Since $P(\text{FA}/E_{ij})$ is symmetric in i and j , i.e.,

$$P(\text{FA}/E_{ij}) = P(\text{FA}/E_{ji})$$

for each i and j , no loss in generality results in restricting $j \geq i$. With this assumption

$$P(\text{FA}/E_{ij}) = 1 - \frac{(N-i)!(N-j)!}{N! [N-(i+j)]!}, \quad (\text{B-4})$$

otherwise the indices i and j are interchanged.

Because we have assumed that the events in $r_1(t)$ are independent of the events in $r_2(t)$, the joint probabilities of the events in $r_1(t)$ and $r_2(t)$ factor, i.e., $P(E_{ij}) = P(E_i) P(E_j)$. If i and j are ≤ 2 , then

$$P(E_{ij}) = \binom{N}{i} \binom{N}{j} p^{i+j} (1-p)^{2N-(i+j)}, \quad (B-5)$$

where if $i = 3$ and $j \leq 2$ then

$$P(E_{ij}) = \left[1 - \sum_{n=0}^2 \binom{N}{n} p^n (1-p)^{N-n} \right] \binom{N}{j} p^j (1-p)^{N-j}. \quad (B-6)$$

Similar results occur if $j = 3$ and $i \leq 2$ and when $i = j = 3$, therefore combining the results of equations (B-3), (B-4), (B-5), and (B-6) result in:

$$\begin{aligned} P_{FA} &= (1-p)^{2N} \sum_{i=1}^2 \sum_{j=1}^2 \left[\binom{N}{i} \binom{N}{j} \left(\frac{p}{1-p} \right)^{i+j} \right] \left[1 - \frac{(N-j)!(N-j)!}{N![(N-i)!]} \right] \\ &\quad + 2 \left[1 - \sum_{n=0}^2 \binom{N}{n} p^n (1-p)^{N-n} \right] \sum_{i=1}^2 \binom{N}{i} p^i (1-p)^{N-i} \left[1 - \frac{(N-3)!(N-i)!}{N![(N-3-i)!]} \right] \\ &\quad + \left[1 - \sum_{n=0}^2 \binom{N}{n} p^n (1-p)^{N-n} \right]^2 \left[1 - \frac{(N-3)^2}{N![(N-6)!]} \right]. \end{aligned} \quad (B-7)$$

A program called "FALSE" is provided (figure B2), which computes the probability of false alarm. On the following page a printout (figure B3) of this program is listed for 10 consecutive thresholds of 1 to 10 rms. This program computes the P_{FA} for each threshold in three separate stages, where each stage corresponds to one of the three cumulative terms of equation B-7. Hence the printout which displays 3 P_{FA} for each threshold shows not only the cumulative effect of the program but also the significance of each term.

For thresholds 1 and 2 rms the last term is the most significant. But as the threshold varies from 2 to 4 rms the largest contribution shifts from the last term to the first term. Unfortunately the region of interest in this report is the transitional region where all the terms contribute.

```

50 OPEN "GD1" FOR OUTPUT AS FILE #1
100 N=60
105 FOR R=1 TO 10
106 T=SQR(2)*P
107 PRINT #1;"THRESHOLD="T
108 PRINT #1;
110 P=EXP(-T)
120 A=1 ~ B=1 ~ C=1 ~ D=1 ~ E=0
125 D=N
130 FOR I=1 TO 2
140 F=0#P/(1-P)/I
145 B=(N+1)*B
146 C=1
147 K=1
148 D=B
150 FOR J=1 TO 2
151 K=K*J
152 C=C*(N-J+1)
154 D=D*(N-(I+J)+1)
156 E=P^J/(1-P)^(J-1)*A*(B/C-D)+E
160 NEXT J
170 NEXT I
180 F=(1-P)^(2*N)*E
200 PRINT #1;"PFA="F
205 K=0
207 J=1*(N+1)
210 FOR I=0 TO 2
230 G=(1-P)^N
240 H=(P/(1-P))^I
250 J=J*(N+1-I)
260 IF I<2 THEN 300
270 J=J/2
300 K=K+J*H*G
310 NEXT I
315 M=1-K
317 C=1
318 A=1
320 FOR J=1 TO 2
330 A=(N+1-J)*A/J
340 B=(P/(1-P))^(J-1)*G
350 C=(N-2-J)/(N+1-J)*C
360 D=1-C
370 F=F+2*A*B*D*M
380 NEXT J
400 PRINT #1;"PFA="F
405 Q=M~2*(1-(N-3)*(N-4)*(N-5)/(N)/(N-1)/(N-2))
500 F=Q+F
600 PRINT #1;"PFA="F
605 NEXT R
610 PRINT #1;
620 PRINT #1;
625 CLOSE
630 END

```

Figure B2. False: A program to compute P_{FA} as a function of rms.

THRESHOLD= 1.41421 - 1 rms
 PFA= 7.44386E-12
 PFA= 2.08732E-06
 PFA= .144943
 THRESHOLD= 2.82843 - 2 rms
 PFA= 3.48577E-03
 PFA= .0349813
 PFA= .105229
 THRESHOLD= 4.24264 - 3 rms
 PFA= 7.75567E-03
 PFA= .0115137
 PFA= .0119598
 THRESHOLD= 5.65685 - 4 rms
 PFA= 7.05532E-04
 PFA= 7.31329E-04
 PFA= 7.31558E-04
 THRESHOLD= 7.07107 - 5 rms
 PFA= 4.31770E-05
 PFA= 4.32799E-05
 PFA= 4.32799E-05
 THRESHOLD= 8.48528 - 6 rms
 PFA= 2.55780E-06
 PFA= 2.55817E-06
 PFA= 2.55817E-06
 THRESHOLD= 9.8995 - 7 rms
 PFA= 1.51201E-07
 PFA= 1.51203E-07
 PFA= 1.51203E-07
 THRESHOLD= 11.3137 - 8 rms
 PFA= 8.93694E-09
 PFA= 8.93694E-09
 PFA= 8.93694E-09
 THRESHOLD= 12.7279 - 9 rms
 PFA= 5.28225E-10
 PFA= 5.28225E-10
 PFA= 5.28225E-10
 THRESHOLD= 14.1421 - 10 rms
 PFA= 3.12211E-11
 PFA= 3.12211E-11
 PFA= 3.12211E-11

Figure B3. Printout of numerical values of the P_{FA} for the threshold varying between 1 and 10 rms.

APPENDIX C
PROBABILITY OF DETECTION

APPENDIX C PROBABILITY OF DETECTION

DERIVATION OF PROBABILITY OF DETECTION

Assume that only one signal is present in the sampling interval, i.e., no multipath exists. Assume this signal is present with signal-to-noise ratio $2E/N_0 = d^2$ in the k' position and that the k' position is one of the N independent sample positions. The probability of detection is the probability that the k' position is ranked in the top three by amplitude in both $r_1(t)$ and $r_2(t)$, where ranked is defined as being greater than the threshold. The probability density function of the amplitude of the k' position, $r_{k'}$, is given by the Rician distribution, i.e.,

$$f_s(r_{k'}) = \frac{r_{k'}}{\sigma^2} \exp \left[-\frac{1}{2\sigma^2} (r_{k'}^2 + a^2) \right] I_0 \left(\frac{a r_{k'}}{\sigma^2} \right) \quad (C-1)$$

where $d^2 = \frac{a^2}{\sigma^2}$ and I_0 is a zeroth order modified Bessel function.

Because only SWGN noise is present in the other ($N-1$) sample positions, the probability density function of these samples is given by the Rayleigh distribution, i.e.,

$$f_n(r_k) = \frac{r_k}{\sigma^2} \exp \left[-\frac{r_k^2}{2\sigma^2} \right] \quad (C-2)$$

Therefore the probability that a noise sample will be greater than a fixed signal amplitude, $r_{k'_0}$, given in equation C-3,

$$P(r_{k'_0}) = P(r_k > r_{k'_0}) = \int_{r_{k'_0}}^{\infty} f_n(r_k) dr_k = e^{-r_{k'_0}^2/2\sigma^2}, \quad (C-3)$$

can be combined with the binomial distribution to give a "list of L"** decision scheme. That is, the probability the $\ell-1$ noise samples out of N samples will be greater than the fixed signal amplitude is the ℓ th term in the binomial expansion with N and $P(r_{k'_0})$ as parameters.

Denote the probability that the signal sample at k' is ℓ th in the list according to amplitude given that the signal amplitude is fixed at $r_{k'_0}$ by

$$P(r_{k'} = \ell^{\text{th}} | r_{k'} = r_{k'_0}).$$

Since

$$P(r_{k'} = \ell^{\text{th}} | r_{k'} = r_{k'_0}) = \binom{N-1}{\ell-1} \left[P(r_{k'_0}) \right]^{\ell-1} \left[1 - P(r_{k'_0}) \right]^{N-\ell}. \quad (C-4)$$

* A notation problem exists between upper case L and lower case ℓ . Upper case is commonly used in the literature, but we have used ℓ instead because ℓ is also a summation index.

it follows that $p(r_{k'} = \ell^{\text{th}})$ is computed by averaging equation C-4 over all $r_{k'_0}$, i.e.,

$$\begin{aligned}
 P(r_{k'} = \ell^{\text{th}}) &= \int_{-\infty}^{\infty} P(r_{k'} = \ell^{\text{th}} | r_{k'} = r_{k'_0}) f_s(r_{k'_0}) dr_{k'_0} \\
 &= \int_{-\infty}^T P(r_{k'} = \ell^{\text{th}} | r_{k'} = r_{k'_0}) f_s(r_{k'_0}) dr_{k'_0} \\
 &\quad + \int_T^{\infty} P(r_{k'} = \ell^{\text{th}} | r_{k'} = r_{k'_0}) f_s(r_{k'_0}) dr_{k'_0}. \tag{C-5}
 \end{aligned}$$

The second integral in equation C-5 has been judiciously chosen to denote the ranked part of the "list of L" decision scheme. Hence, the second integral of equation C-5,

$$\begin{aligned}
 P(r_{k'} = \ell^{\text{th}} \text{ and } r_{k'} \text{ is ranked}) &= P(r_{k'} \text{ is ranked } \ell^{\text{th}}) \\
 &= \int_T^{\infty} P(r_{k'} = \ell^{\text{th}} | r_{k'} = r_{k'_0}) f_s(r_{k'_0}) dr_{k'_0}, \tag{C-6}
 \end{aligned}$$

is just the integral necessary in computing the probability of detection. This integral can be expressed in terms of the "Marcum Q-function," defined as

$$Q(\alpha, \beta) \triangleq \int_{\beta}^{\infty} r \exp\{-\frac{1}{2}(r^2 + \alpha^2)\} I_0(\alpha r) dr.$$

Substituting equation C-3 into equation C-4 and then equation C-4 and equation C-1 into equation C-6 results in the cumbersome equation C-7,

$$\begin{aligned}
 P(r_{k'} \text{ is ranked } \ell^{\text{th}}) &= \int_T^{\infty} \binom{N-1}{\ell-1} \left[e^{-r_{k'_0}^2/2\sigma^2} \right]^{\ell-1} \left[e^{-r_{k'_0}^2/2\sigma^2} \right]^{N-\ell} \frac{r_{k'_0}}{\sigma^2} \\
 &\quad \exp \left[\frac{-(r_{k'_0}^2 + \alpha^2)}{2\sigma^2} \right] I_0 \left(\frac{\alpha r_{k'_0}}{\sigma^2} \right) dr_{k'_0}. \tag{C-7}
 \end{aligned}$$

To simplify equation C-7, without loss of generality, make the following substitutions:
(1) $r = r_{k'} \frac{o}{\sigma}$; (2) $ba = T$ where b is an arbitrary positive constant; (3) express the

binomial, $[1 - e^{-r^2/2}]^{N-\ell}$, in terms of its expansion,

$\sum_{j=0}^{N-\ell} (-1)^j \binom{N-\ell}{j} e^{-jr^2/2}$; and (4) let $d^2 = a^2/\sigma^2$. With these changes equation C-7 becomes

$$P(r_{k'} \text{ is ranked } \ell^{\text{th}}) = e^{-d^2/2} \int_0^\infty \binom{N-1}{\ell-1} \sum_{j=0}^{N-\ell} \binom{N-\ell}{j} (-1)^j e^{\frac{-r^2(\ell+j)}{2}} I_o(rd) r dr. \quad (\text{C-8})$$

Now equation C-8 can be evaluated in terms of the "Q-function" by recombining terms and substituting x for $\sqrt{\ell+j} r$, i.e.,

$$\begin{aligned} P(r_{k'} \text{ is ranked } \ell^{\text{th}}) &= e^{-d^2/2} \binom{N-1}{\ell-1} \sum_{j=0}^{N-\ell} e^{\frac{d^2}{2(\ell+j)}} \frac{(-1)^j \binom{N-\ell}{j}}{(\ell+j)} \int_{\sqrt{\ell+j} b}^\infty \\ &\quad e^{-\frac{1}{2} \left(x^2 + \frac{d^2}{\ell+j} \right)} I_o \left(\frac{xd}{\sqrt{\ell+j}} \right) x dx \\ &= e^{-\frac{d^2}{2}} \binom{N-\ell}{\ell-1} \sum_{j=0}^{N-\ell} e^{\frac{d^2}{2(\ell+j)}} \binom{N-\ell}{j} \frac{(-1)^j}{(\ell+j)} Q \left(\frac{d}{\sqrt{\ell+j}}, b \sqrt{\ell+j} \right) \end{aligned} \quad (\text{C-9})$$

It follows that the probability that the k' position is ranked in the top three positions, i.e., $\ell=1, 2$, and 3 , as just a sum on equation C-9 from $\ell=1$ to 3 , i.e., $P(r_{k'} \text{ is ranked in top three positions}) =$

$$\sum_{\ell=1}^3 \binom{N-1}{\ell-1} \sum_{j=0}^{N-\ell} \binom{N-\ell}{j} \left(\frac{-1}{\ell+j}\right)^j e^{-\frac{d^2}{2}} \left(1 - \frac{1}{\ell+j}\right) Q(d/\sqrt{\ell+j}, b\sqrt{\ell+j}) \quad (C-10)$$

Finally the probability of detection is equation C-10 squared, since the k' position in $r_1(t)$ is independent of the k' position in $r_2(t)$. Therefore the probability of detection is given as:

$$P_D = \left\{ \sum_{\ell=1}^3 \binom{N-1}{\ell-1} \sum_{j=0}^{N-\ell} \binom{N-\ell}{j} e^{-\frac{d^2}{2}} \left(1 - \frac{1}{\ell+j}\right) \frac{(-1)^j}{(\ell+j)} Q(d/\sqrt{\ell+j}, b\sqrt{\ell+j}) \right\}^2 \quad (C-11)$$

COMPUTATION OF THE PROBABILITY OF DETECTION

Computing the probability of detection, as given in equation C-11 with $b=2$ * would not only require calculating virtually $3N$ "Q-functions" and $3N$ binomial coefficients, but also determining the accuracy of such a calculation would be difficult. Therefore two independent methods for computing equation C-11 are presented and compared. First, the double sum of equation C-11 is reduced to a single sum of only $N/2$ computations and then computed directly. Next, the original integral equation is numerically integrated using the trapezoidal rule.

DIRECT COMPUTATION

The double sum in equation C-11 is reduced to a single sum by introducing the variable k for $\ell + j$, interchanging the order of summation, and then evaluating the inner summation in terms of K . The resulting expression for the probability of detection is given in equation C-12.

$$P_D = \left\{ \sum_{k=1}^N (-1)^{k-1} \binom{N-1}{k-1} \frac{(k-2)(k-3)}{2k} e^{-d^2/2(1-1/k)} Q(d/\sqrt{k}, 2\sqrt{k}) \right\}^2 \quad (C-12)$$

The major contribution to this sum is the first term, $Q(d, 2)$, which is the probability of detecting a signal of unknown phase in SWGN. For fixed d and $k \ll d^2$, $Q(d/\sqrt{k}, 2\sqrt{k})$

* Setting the threshold at $b=2$ corresponds to a threshold of 3 dB above the rms noise level. Even though we have restricted our computation to this level in this section, results for a variable threshold are given in the results section.

approaches zero like $e^{-1/2(2\sqrt{k})^2} = e^{-2k}$. Note the threshold, in this case 2, is the coefficient of the \sqrt{k} in the second argument of the "Q-function." Since the binomial coefficient $\binom{N-1}{k-1}$ has its maximum at approximately $k=N/2$, the contributions to the sum will significantly decrease for $k > N/2$. Therefore, since we have an alternating series, the error introduced by truncating the summation at $k=N/2$ will be bounded by the contribution at $k=N/2$. The binomial coefficient at $N/2$ is asymptotically equal to $\frac{e^{N\ln 2}}{\sqrt{2\pi N}}$. Combining the approximations for the binomial coefficient, the "Q-function" and the rest of the multipliers at $k=N/2$ results in a contribution of $\frac{\sqrt{N}e^{N(\ln 2 - 1)}}{10}$. For $N=60$ this is $O(10^{-8})$.

If we include the normalized threshold in this expression and restrict $N \geq 60$ then the error introduced by truncating at $k=N/2$ is

$$\sim \frac{\sqrt{N}}{10} e^{N(\ln 2 - T^2/4)} \text{ which is } O(10^{-8}) \text{ for } T \geq 2.$$

The "Q-functions were computed either recursively⁽¹⁾ or asymptotically⁽²⁾ depending on the $|d/\sqrt{k} - 2\sqrt{k}|$. Substituting Dillard's recursive formula in equation C-12 and cancelling where necessary results in

$$P_D = \left\{ \sum_{k=1}^N (-1)^{k-1} \binom{N-1}{k-1} \frac{(k-2)(k-3)}{2k} e^{-\left(\frac{d^2}{2} + 2k\right)} \sum_{j=0}^{\infty} \frac{\left(\frac{d^2}{2k}\right)^j}{j!} \sum_{l=0}^j \frac{(2k)^l}{l!} \right\}^2.$$

The infinite sum on j may be truncated by lower bounding M^{th} term. For $j=M$ and $M \gg 1$

we have the M^{th} term in the j^{th} summation $\sim \left(\frac{ed^2}{M}\right)^M$. Given $d=2$ and $M=30$, this term $\sim 10^{-14}$. When $d=3$ and $M=40$ this term $\sim 10^{-9}$.

NUMERICAL INTEGRATION

The probability of detection may be computed numerically by transforming the integrals of equation C-13.

$$P_D = \left\{ e^{-d^2/2} \sum_{k=1}^3 \binom{N-1}{k-1} \int_2^\infty e^{-kx^2/2} x \left(1-e^{-x^2/2}\right)^{N-k} I_0(xd) dx \right\}^2. \quad (\text{C-13})$$

This integral can be efficiently evaluated by the trapezoidal rule after several changes of variables. Substituting $u=e^{-x^2/2}$ and changing limits of integration transforms the integral to one of Rice's⁽³⁾ examples. Let I represent the integral of equation C-13. Then

$$I = \int_0^{e^{-2}} u^{k-1} (1-u)^{N-k} I_0(\sqrt{-2\ell n u} d) du. \quad (C-14)$$

Identifying equation C-14 with equation C-9, of reference (3) immediately yields the following transformations

$$u = e^{-2}/(1 + e^{-2v}) \quad (C-15)$$

$$\frac{du}{dv} = 2ue^2(e^{-2}-u) \quad (C-16)$$

$$\frac{dv}{dx} = \frac{3}{4} \left(e^x + \frac{e^{-x}}{k} \right) \quad (C-17)$$

After making these transformations, equation C-14 can be written as a function of x.

$$I = \frac{3}{2} e^2 \int_{-\infty}^{\infty} u^k (e^{-2}-u) (1-u)^{N-k} I_0(\sqrt{-2\ell n u} d) \left(e^x + \frac{e^{-x}}{k} \right) dx$$

Even though x goes from $-\infty$ to ∞ , the exponential terms rapidly decrease both tails significantly. In fact six significant figures can be achieved by taking only 24 points from $x = -4$ to 4 in steps of .32.

A comparison of the numerical integration and the summation can be found in table C1. Only one threshold is shown in this table but similar results exist at larger thresholds, e.g., $T = 2\sqrt{2}\sigma$. Table C-1 clearly shows agreement to a minimum of three significant figures and better agreement as the SNR increases. Therefore confidence exists in using the summation method.

Flow diagrams with program listings are provided for both the summation method and the numerical integration method in figures C1, C2, C3, and C4. This program is general for any threshold and any SNR. But computation for SNR much greater than 15 dB gives erroneous results in both cases. An attempt at upper and lower bounding the P_D at a threshold of 3 dB above the rms value was unsuccessful at higher SNR. This approach will be attempted using a threshold setting greater than 10 dB where the P_D is no longer almost 1.

Table C-1. Threshold set at 3 dB above the rms noise. False alarm rate = .144636.

SNR	SUMMATION METHOD	NUMERICAL INTEGRATION
5	.340613	.340441
6	.476614	.476438
7	.629841	.629868
8	.777143	.777162
9	.891837	.891847
10	.960402	.960406
11	.989929	.989929
12	.998398	.998398
13	.999861	.999861
14	.999995	.999994
15	1	.999999

Note: SNR is measured in dB.

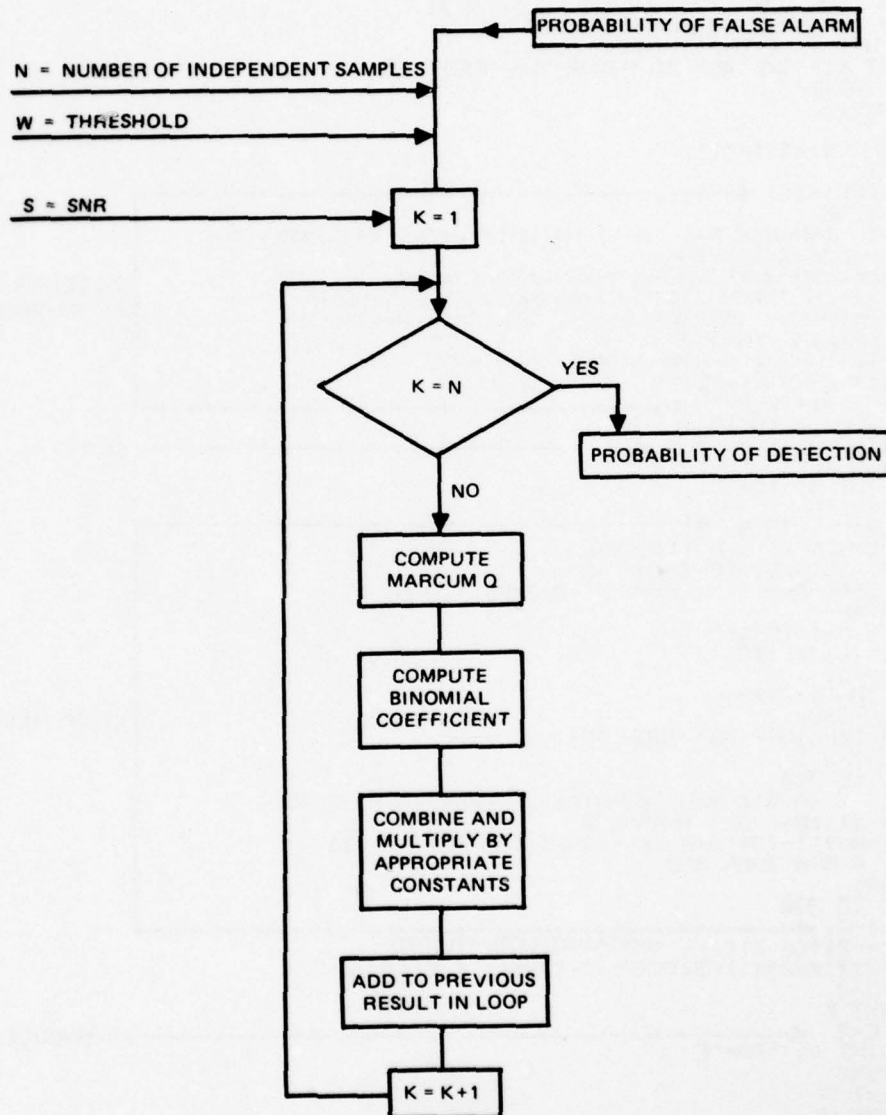


Figure C1.

```

3 OPEN "ANS.DAT" FOR OUTPUT AS FILE #1
5 N=60   #OF INDEPENDENT SAMPLES
7 FOR W=1 TO 2 THRESHOLDS
8 PRINT #1;"THE #OF SD ABOVE THE NOSIE IS" W
10 S1=SQR(2)
15 T=W*S1
16 T1=T
17 PRINT #1;"T1="T1,
20 T1=T
21 X2=EXP(-T1) ←
22 X1=1-X2
23 X3=1-X1^N-N*X2*X1^(N-1)-N*(N-1)/2*(X2/X1)^2*X1^(N-2)
25 Y1=N*X2^2*X1^(2*N-2)
30 Y2=N*(2*N-3)*(2*N-2)/4*X2^4*X1^(2*N-4)
35 Y3=(1-(N-3)*(N-4)*(N-5)/N/(N-1)/(N-2))*X3^2
40 Y4=2*(N*(N-1)*X2^2*X1^(N-2)*(X2*X1^(N-1)+X3))
45 Y5=6*X2*X1^(N-1)*X3
50 Y6=-2*(N-3)*(N-4)*X2^2*X1^(N-2)*X3
60 P=Y1+Y2+Y3+Y4+Y5+Y6
65 PRINT #1;"PFA="P ←
100 FOR S=10 TO 15
103 PRINT #1;"SNR="S, ← SNR
105 D=SQR(2*X10^(S/10))
107 PRINT #1;"D="D,
110 Z1=-1/N \ C=0
120 FOR K=1 TO N ←
150 A=D/SQR(K) \ B=T1*SQR(K)
155 IF ABS(A-B)>10 THEN 252
160 F=EXP(-A^2/2) \ D1=EXP(-B^2/2) \ H=D1
170 Q=F*XH
180 FOR J=1 TO 100
190 D1=(B^2/2)*D1/J
200 H=H+D1
210 F=(A^2)/2*F/J
220 Q=Q+F*XH
230 IF F*XH<10^(-20) THEN 251
240 NEXT J
245 GO TO 270
251 Q1=-1/(A-B)*(B/6.28318*A)^.5*EXP(-(A-B)^2/2)
253 IF Q1<10^(-32) THEN 430
254 Q1=Q1*(1-(3*(A+B)^2-4*B^2)/(8*A*B*(A-B)))
255 IF A-B>0 THEN 260
256 Q=Q1
257 GO TO 270
260 Q=1-Q1 ←
270 Z1=-Z1*(N-K+1)/K BINOMIAL COEFFICIENT
280 C=Z1*(K-2)*(K-3)*EXP(-D^2/2*(1-1/K))*Q/2+C
285 P=C^2
295 NEXT K
300 P=C^2 ←
340 PRINT #1;"PD="P ← PROBABILITY OF DETECTION
341 PRINT
350 NEXT S
355 NEXT W
358 CLOSE
460 END

```

ALTERNATIVE COMPUTATIONS
OF PROBABILITY OF FALSE ALARM

COMPUTES MARCUM Q - FUNCTIONS

PROBABILITY OF DETECTION

Figure C2. Summation method.

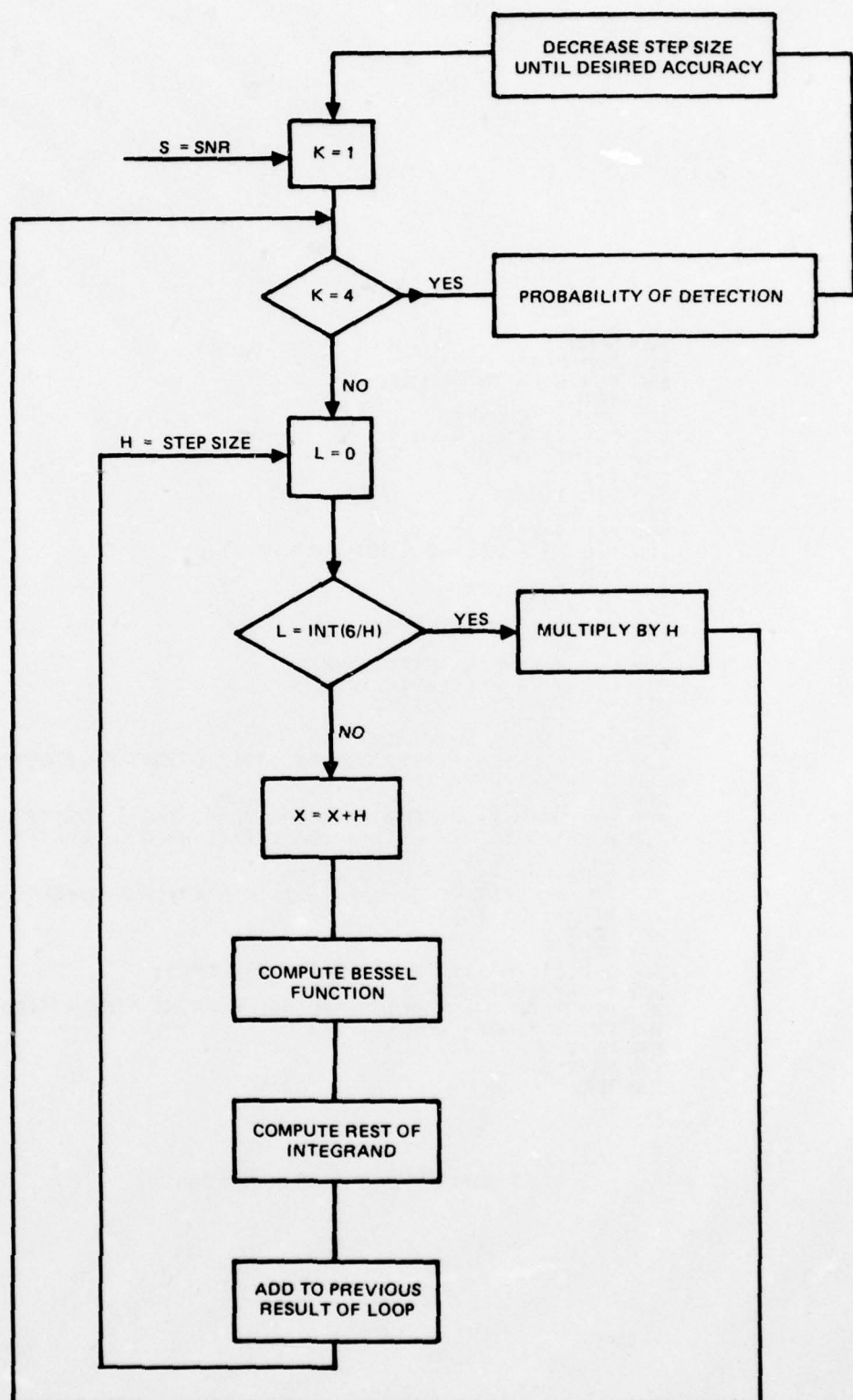


Figure C3.

```

100 N=60
110 DIM P(4)
120 FOR S=10 TO 20 STEP 5
121 PRINT
122 PRINT "SNR="S,
125 D=SQR(2*10^(S/10))
127 PRINT "D="D
130 I=0
140 DIM I(805)
150 H=.64
160 FOR J=1 TO 3
165 P(0)=0 \ P(1)=0 \ P(2)=0 \ P(3)=0
170 H=H/2
180 FOR K=1 TO 3
185 X=-3.5-H
190 FOR L=0 TO INT(7/H)
195 X=X+H
200 U=3/4*(EXP(X)-EXP(-X)/K)
210 U=EXP(-2)/(1+EXP(-2*U))
215 X1=SQR(-2*LOG(U))*D
217 T=X1/3.75
220 IF X1>3.75 THEN 260
230 B1=1+3.51562*T^2+3.08994*T^4+1.20675*T^6+.265973*T^8
240 B=B*EXP(-D^2/2)
250 GO TO 300
260 B1=.398942+.0132859/T+4.40067E-03/T^2-1.57565E-03/T^3
270 B2=B1+9.16281E-03/T^4-.0205771/T^5+.0263554/T^6-.0164763/T^7
280 B3=B2+3.92377E-03/T^8
290 B=B3*EXP(X1-D^2/2)/SQR(X1)
300 I(L)=U^K*(EXP(-2-U)*(1-U)^(N-K)*B*(EXP(X)+EXP(-X)/K)
310 P(K)=I(L)+P(K)
320 NEXT L
330 NEXT K
340 Q=P(1)+(N-1)*P(2)+(N-1)*(N-2)/2*P(3)
350 R=(EXP(2)*3/2*H^20)^2
360 PRINT "H="H\ PRINT "PD="R\ PRINT "IMIN="I(0);
365 PRINT "IMAX="I(INT(7/H)))
380 NEXT J
385 NEXT S
390 END
--
```

Figure C4. Numerical integration.

REFERENCES TO APPENDIX C

1. George M. Dillard, "Recursive Computation of the Generalized Q-function," IEEE Trans, on Aerospace and Electronic Systems, Vol.-9 number 4 July 1973.
2. S. O. Rice, "Mathematical Analysis of Random Noise," Selected Papers on Noise and Stochastic Processes, N. Wax, Ed. New York: Dover, 1954.
3. S. O. Rice, "Efficient Evaluation of Integrals of Analytic Functions by the Trapezoidal Rule," B.S.T.J., 52, No. 5 (May-June 1973), pp. 707-722.

APPENDIX D
TIME OF ARRIVAL ESTIMATION ERROR FOR OPTIMUM DETECTION

APPENDIX D

TIME OF ARRIVAL ESTIMATION ERROR FOR OPTIMUM DETECTION

The basic equation for pulse resolution in white noise is worked out by Helstrom, Carl, Statistical Theory of Signal Detection, 2nd Edition; 1968, and is given by

$$\text{Var } \hat{\tau} = \frac{1}{d^2 (\Delta W)^2}$$

where

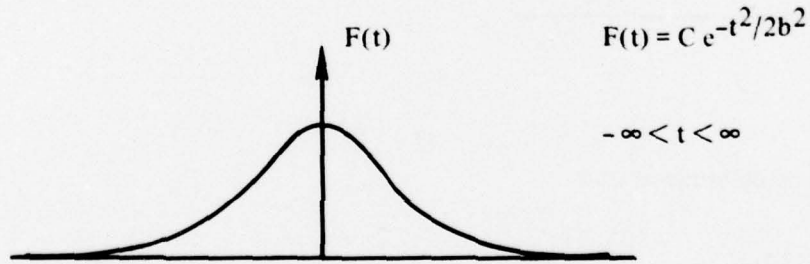
$$d^2 = \frac{2E}{N_0}, (\Delta W)^2 = \int_{-T/2}^{T/2} |F'(t)|^2 dt$$

and

$$\int_{-T/2}^{T/2} |F(t)|^2 dt = 1.$$

The pulse resolution of three different pulse shapes will be considered, a Gaussian, cosine square, and a modified rectangular pulse with cosine square rise and fall. The modified rectangle pulse will be used as an approximation to the sounder pulse.

Case I Gaussian Pulse



The constant C is determined by

$$\int_{-\infty}^{\infty} |F(t)|^2 dt = 1$$

$$C^2 \int_{-\infty}^{\infty} e^{-t^2/b^2} dt = C^2 b \sqrt{\pi} = 1 \therefore C = b^{-1/2} \pi^{-1/4}$$

The bandwidth, then, is

$$(\Delta W)^2 = \int_{-\infty}^{\infty} |F'(t)|^2 dt = \frac{C^2}{b^4} \int_{-\infty}^{\infty} t^2 e^{-t^2/b^2} dt$$

$$(\Delta W)^2 = \frac{1}{2b^2}$$

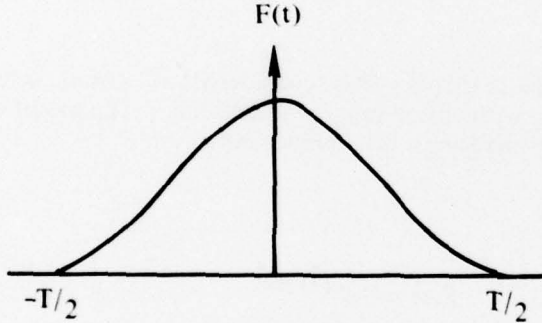
Substituting $\text{Var } \hat{\tau} = 2b^2/d^2$,

and thus $\sqrt{\text{Var } \hat{\tau}} = \text{rms error} = \frac{\sqrt{2b}}{d}$

The error is directly proportional to the pulse width and inversely proportional to signal-to-noise ratio.

Case II Cosine Square Pulse

$$F(t) = A \cos^2 \frac{\pi t}{T}$$



The constant A can be determined from

$$\int_{-\infty}^{\infty} |F(t)|^2 dt = 1$$

$$A^2 \int_{-T/2}^{T/2} \cos^4 \frac{\pi t}{T} dt = 1$$

Using integral equation #304, page 429 of the 17th edition of CRC gives

$$A^2 \left[\frac{3t}{8} + \frac{\sin 2(\frac{\pi}{T})t}{\frac{4\pi}{T}} + \frac{\sin 4(\frac{\pi}{T})t}{32(\frac{\pi}{T})} \right] \Big|_{-T/2}^{T/2}$$

resulting in

$$A = \sqrt{\frac{8}{3T}}$$

The bandwidth ΔW is given by

$$(\Delta W)^2 = \int_{-T/2}^{T/2} |F'(t)|^2 dt$$

where

$$F'(t) = -\frac{2A\pi}{T} \cos\left(\frac{\pi t}{T}\right) \sin\left(\frac{\pi t}{T}\right)$$

Substituting

$$(\Delta W)^2 = \frac{4\pi^2}{3T^2}$$

the variance is then

$$\text{Var } \hat{r} = \frac{1}{d^2 \left(\frac{4\pi^2}{3T^2} \right)}$$

which gives an rms error of

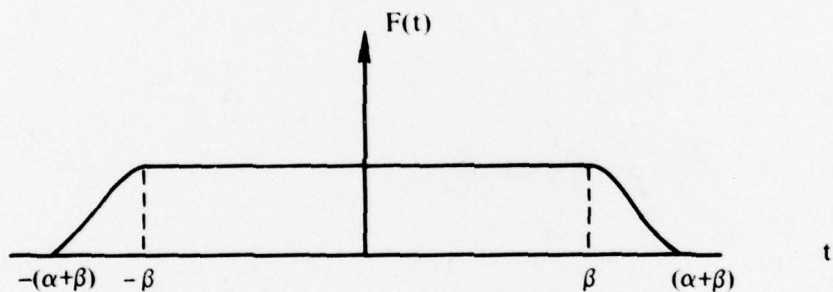
$$\frac{\sqrt{3}}{2\pi} \frac{T}{d}$$

RMS error for Cosine Square Pulse.

SNR, dB	T, the Pulse Width		
	0.01 msec	0.1 msec	1.0 msec
0	2.754	27.57	275.7
10	0.8718	8.718	87.18
20	0.2757	2.757	27.57
30	0.087	0.8718	8.718
40	0.027	0.2757	2.757
50	0.008	0.087	0.8718
60	0.0027	0.027	0.2757

Case III Sounder Pulse

$$F(t) = \begin{cases} A \cos^2 \frac{\pi}{2\alpha} (t+B) & -(\alpha+B) \leq t \leq -\beta \\ A & -\beta \leq t \leq \beta \\ A \cos^2 \frac{\pi}{2\alpha} (t+B) & \alpha \leq t \leq (\alpha+B) \end{cases}$$



A is determined by

$$\int_{-T/2}^{T/2} |F(t)|^2 dt = 1$$

which gives

$$A = \left(\frac{3\alpha}{4} + 2\beta \right)^{-1/2}$$

The pulse bandwidth ΔW (in radians) is given by

$$(\Delta W)^2 = \int_{-T/2}^{T/2} |F'(t)|^2 dt$$

where

$$F'(t) \begin{cases} -2A \cos \frac{\pi}{2\alpha}(t+\beta) \sin \frac{\pi}{2\alpha}(t+\beta) \left(\frac{\pi}{2\alpha} \right) & -(\alpha+\beta) \leq t \leq -\beta \\ 0 & -\beta \leq t \leq \beta \\ -2A \cos \frac{\pi}{2\alpha}(t-\beta) \sin \frac{\pi}{2\alpha}(t-\beta) \left(\frac{\pi}{2\alpha} \right) & \beta \leq t \leq (\alpha+\beta) \end{cases}$$

Substituting and integrating gives

$$(\Delta W)^2 = \frac{(\pi/2)^2}{\left(\frac{3\alpha}{4} + 2\beta \right) \alpha}$$

The time of arrival variance is then

$$\text{Var } \hat{\tau} = \frac{\alpha \left(\frac{3\alpha}{4} + 2\beta \right)}{d^2 (\pi/2)^2}$$

which gives an rms error of

$$\text{rms error} = \sqrt{\frac{\alpha \left(\frac{3\alpha}{4} + 2\beta \right)}{\pi/2 d}}$$

For the NTSS sounder pulse we have

$$\alpha = 20 \times 10^{-6} \text{ seconds}$$

$$\beta = 80 \times 10^{-6} \text{ seconds}$$

$$\text{rms error} = \frac{9.416 \times 10^{-6}}{d}$$

	SNR, * dB	rms error microseconds
$*\text{SNR} = \frac{2E_s}{N_o}$	0	37.6629
	10	11.9101
	20	03.7663
	30	01.1901
	40	00.3766
	50	00.1901

APPENDIX E

**STATISTICS OF THE RMS ESTIMATOR AND DETERMINATION OF THRESHOLD
INCREASES NECESSARY TO MAINTAIN A PREDETERMINED FALSE ALARM RATE**

APPENDIX E
STATISTICS OF THE RMS ESTIMATOR AND DETERMINATION OF THRESHOLD
INCREASES NECESSARY TO MAINTAIN A PREDETERMINED FALSE ALARM RATE

The purpose of this appendix is to derive the statistics of the rms noise estimator. With these statistics one can determine the effect of using an estimate, rather than the true rms value, to determine the threshold setting. The criterion used to determine this effect is twofold: (1) increase our estimate of the required threshold until we are certain this increased threshold is at least as large as the required threshold, and (2) determine the increase in signal-to-noise ratio (SNR) required to maintain the prescribed probability of detection (P_D). Since the envelope is Rayleigh distributed with an rms value equal to $\sqrt{2}\sigma$, the expected value of our estimator should approach this value with minimum variance. The estimator we have chosen is

$$S = \sqrt{\frac{1}{N} \sum_{i=1}^N (X_i^2 + Y_i^2)} \quad (E-1)$$

where X_i and Y_i are Gaussian random variables with zero mean and variance σ^2 . Note also that N is the number of independent samples of the envelope.

Using a straightforward transformation of the random variable S to a new random variable $Z = \frac{NS^2}{\sigma^2}$ with a chi-squared distribution of $2N$ degrees of freedom the distribution of S can easily be solved for. The density function of Z is given by

$$f_Z(Z) = \frac{Z^{N-1}}{2^N \Gamma(N)} e^{-Z/2} \quad Z \geq 0$$

$$0 \quad \text{otherwise.} \quad (E-2)$$

Therefore using the identity

$$f_S(S) ds = f_Z(Z) dz$$

or equivalently,

$$f_S(S) = f_Z(Z(S)) \frac{dz}{ds},$$

the density function of S is easily determined to be

$$f_S(S) = \frac{2}{\Gamma(N)} \left(\frac{N}{2\sigma^2} \right)^N S^{2N-1} e^{-\frac{NS^2}{2\sigma^2}} \quad S \geq 0$$

$$0 \quad \text{otherwise.} \quad (E-3)$$

With the density function of S at hand we may easily compute the important moments of S which are listed below:

$$E[S] = \sqrt{2} \sigma \left(1 - \frac{1}{8N} + \frac{1}{128N^2} - \dots\right) \quad (E-4)$$

$$E[S^2] = 2\sigma^2 \quad (E-5)$$

$$\sigma_S = \sqrt{E(S^2) - [E(S)]^2} \approx \frac{\sigma}{\sqrt{2N}} \quad (E-6)$$

Equation E-4 implies that S is asymptotically an unbiased estimator, i.e., as $N \rightarrow \infty$ the $E[S] \rightarrow \sqrt{2}\sigma$ which is the true rms value. Whereas equation E-6 implies that S is asymptotically consistent, or equivalently that $\sigma_S \rightarrow 0$ as $N \rightarrow \infty$. Therefore as long as N is "large," i.e., the sampling window used is sufficiently large, S will provide a "good" estimate of the rms value.

Equation E-3 also provides the information necessary to determine the consequence of raising the threshold. The threshold is set to operate at a predetermined probability of false alarm (P_{FA}). Actual adjustments in the threshold are obtained by adjusting the multipliers of the rms value, b . Hence the threshold is set to $brms = b\sqrt{2}\sigma$ where b is determined by the P_{FA} desired. Therefore variability in our estimate of rms require adjustments to our threshold estimate.

An adjusted estimate of the desired threshold $b\sqrt{2}\sigma$ is αbs where α is determined by $P(\alpha bs \geq b\sqrt{2}\sigma) = 0.98$ for example. That is, determine α such that $\alpha bs \geq b\sqrt{2}\sigma$ with 98% confidence. Of course 98% is an arbitrary value and in addition to the 98% confidence value, alternative confidence values will be used to evaluate α . Rather than numerically integrate equation E-3, transform the arguments of the thresholds so that tabulated values for the chi-squared distributions can be used. Illustrated by equations E-7 to E-10 are the transformations which are used to determine α where $\frac{Ns^2}{\sigma^2}$ is a

$$P(\alpha bs \geq b\sqrt{2}\sigma) = 0.98 \quad (E-7)$$

$$P(\alpha S \geq \sqrt{2}\sigma) = 0.98 \quad (E-8)$$

$$P(\alpha^2 S^2 \geq 2\sigma^2) = 0.98 \quad (E-9)$$

$$P\left(\frac{Ns^2}{\sigma^2} \geq \frac{2N}{\alpha^2}\right) = 0.98 \quad (E-10)$$

chi-squared random variable with $2N$ degrees of freedom.

A conversion of N to milliseconds of sampling window size is accomplished by conversion of 1 millisecond for every $2N = 15$. Using J. Murdock & J. A. Barnes, "Statistical Tables," Halsted Press 2nd Edition: 1970, statistics of the chi-squared distribution up to 100 degrees of freedom are used to plot various values of α . In figure E1, α is plotted for confidence limits of 99%, 98% and 80% with sampling window size from 0 to 7 milliseconds. For each of the confidence values α decreases rapidly as the window size increases to 2 milliseconds. As the window size increases further from 2 to 7 milliseconds only a gradual decrease is noted. In fact the slope approaches zero with intercept one as the window size increases.

These values of α may be used with the results of Appendix C to determine the increase in SNR required to maintain a P_D for a predetermined P_{FA} . Only in combination with the results of Appendix C can a valid determination of an appropriate α be made.

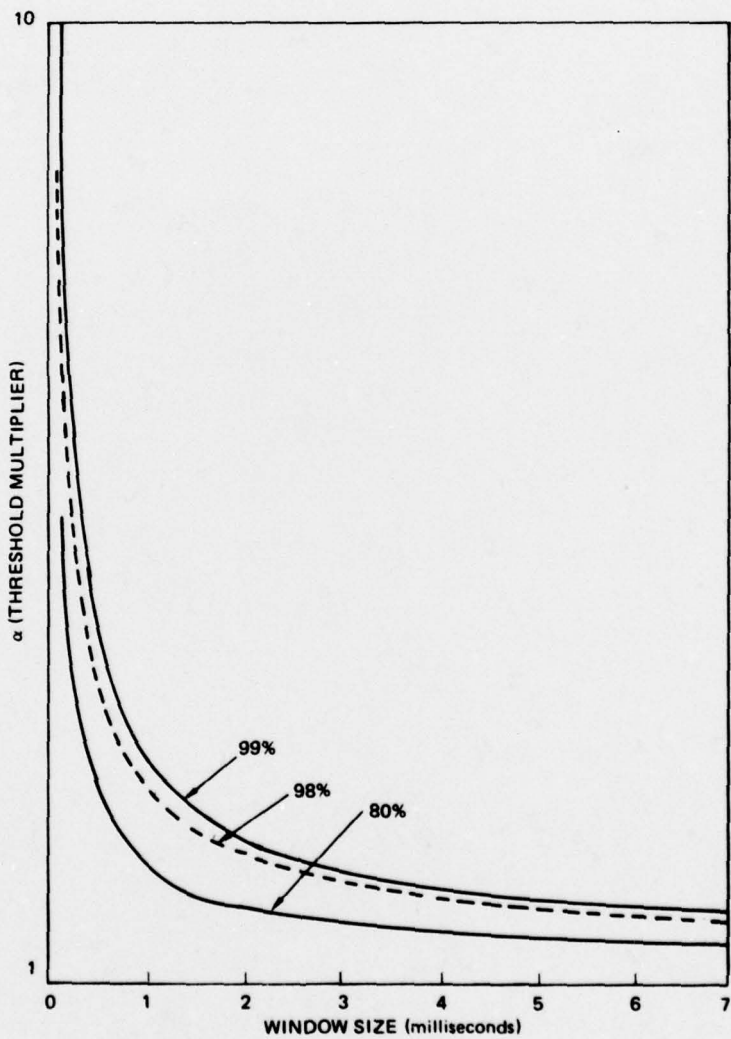


Figure E1. Variation in multiplication of threshold estimate needed to maintain a predetermined P_{FA} .